

Living Near de Sitter Bubble Walls

Jin-Ho Cho^{1,2} and Soonkeon Nam¹

¹*Department of Physics & Research Institute for Basic Sciences,
Kyung Hee University, Seoul 130-701, Korea*

²*Center for Quantum Space Time, Sogang University, Seoul 121-742, Korea*

E-mail: cho.jinho@gmail.com, nam@khu.ac.kr

ABSTRACT: We study various bubble solutions in string/M theories obtained by double Wick rotations of (non-)extremal brane configurations. Typically, the geometry interpolates de Sitter space-time \times non-compact extra-dimensional space in the near-bubble wall region and the asymptotic flat Minkowski space-time. These bubble solutions provide nice background geometries to reconcile string/M theories with de Sitter space-time. For the applications of these solutions to cosmology, we consider multi-bubble solutions and find a landscape of varying cosmological constant. Double Wick rotation in string/M theories introduces imaginary higher-form fields. Rather than regard these fields as *classical* pathologies, we interpret them as *semi-classical* decay processes of de Sitter vacuum via the production of spherical branes. We speculate on the possibility of solving the cosmological constant problem making use of the condensation of the spherical membranes.

KEYWORDS: bubble, de Sitter space-time, string/M-theories, creation of spherical branes, cosmological constant problem.

Contents

1. Introduction	2
1.1 De Sitter Space-time and String Theory	2
1.2 Detouring the No-go theorem in Supergravity	4
1.3 Geometry near the Wall of Witten's Bubble	5
2. D-bubbles and M-bubbles	7
2.1 D/M-brane Configurations and their Bubble Cousins	7
2.2 Near-Bubble Geometries and de Sitter space-time	8
2.3 Exact Near-Bubble Solutions: Extremal Cases	9
3. Multi-Bubbles : Swiss Cheese Universe	12
3.1 Maximal Supersymmetries near the Walls of Extremal Bubbles	12
3.2 Null Geodesic Lines in the Bubble Geometry	14
3.3 Bubble Landscape - Swiss Cheese Universe	15
4. Semi-classical Instability of de Sitter Space-times	18
4.1 The Creation of Spherical M2 Branes in M5-Bubble Background	18
4.2 Spherical M2 Branes and the Cosmological Constant Problem	20
5. Bubble Nucleation	21
5.1 Bubbles vs. Instability of Kaluza-Klein Vacua	21
5.2 Energy Condition of the Bubbles	23
6. Extending Hartle-Hawking to Extra Dimensions	24
7. Discussions	27
A. Action under the Double Wick Rotation (DWR)	30
B. D/M-bubbles from D/M-brane configurations via DWR	31
C. Supersymmetry in the Near-Bubble Geometry: Details	35

1. Introduction

1.1 De Sitter Space-time and String Theory

Nearing the end of last century, astronomers had an astonishing discovery, the universe is expanding with acceleration [1][2]. This discovery called for many new ideas, since the conventional gravity is an attractive force and cannot accelerate the expansion of the Universe.

Positive cosmological constant [3][4][5][6] is the oldest and simplest solution, but for string theorists, poses a daunting problem. De Sitter space-time which is the cosmological solution with positive cosmological constant Λ , does not easily allow string theory in it [7]. The problem is as follows. There is a deep rooted problem of formulating quantum field theory in de Sitter space-time, let alone string theory. The basic reason is that whereas de Sitter space-time only allow finite degrees of freedom, quantum field theory (or string theory) has infinite degrees of freedom. The finiteness of degrees of freedom in de Sitter space-time is related to the fact that it has finite entropy and thus the degrees of freedom in it can only be finite [8][9][10][11][12]. There is no unitary way to act de Sitter group on the finite degrees of freedom.

To make matters worse, there is a ‘no-go theorem’ in string theory (supergravity) which rules out de Sitter space-time as a result of non-singular warped compactification [13]. The basic assumptions for this theorem are i) no higher curvature correction in the gravity action, ii) the non-positive potentials for the scalars, iii) massless fields with positive kinetic terms, and iv) finite effective Newton’s constant in lower dimensions.

In this paper, we study various bubble solutions in string/M theories and their applications to cosmological problems. The bubble solutions have a region, the near-bubble wall region, which is de Sitter, but asymptotically are flat Minkowski. Therefore, they have plenty of rooms to allow infinite degrees of freedom of string theory. Moreover, we will argue that most matters are accumulated near the bubble wall as the bubble expands. Therefore most of the galaxies are formed near the bubble wall and it is natural that intelligent observers see de Sitter space-time around them.

These solutions are obtained by performing the double Wick rotation (DWR) on well-known D/M-brane solutions and we will call them D/M-bubbles. First, we find that near the bubble wall, the geometry becomes ‘de Sitter \times non-compact internal space’. Second, we find that the case of extremal D3-bubble corresponds to Hull’s Euclidean brane (called E4-brane) [14]. However, other cases we have considered, such as M2- or M5-bubbles are new and cannot be obtained by Hull’s timelike T-duality of type II theories because there is no notion of T-duality in M theory.

Extremal D3-bubbles (including M2- and M5-bubbles) preserve full 32 supersymmetries near the bubble wall and at the asymptotic infinity. In order to make sense of supersymmetry in this background, Ramond-Ramond (RR) should be imag-

inary, which is also a consequence of DWR. Imaginary valued fields, at least for free cases, can be regarded as fields with the wrong sign for the kinetic term. At first glance, this might sound pathological. However, there is a long history of fields with the wrong kinetic term [15][16], and recently such fields have been considered as the candidate for the dark energy [17] which are the source for the acceleration of the expansion of the Universe. (However, certain problems about the kinetic terms with wrong sign have been pointed out in view of phenomenology [18].)

In this paper, we *assume the imaginary valued fields at the semi-classical level* and pursue the foregoing argument about de Sitter space-time in 10- or 11-dimensional supergravity. Although this scheme is quite against the standard folklore, one should have checked at least whether it leads to any inconsistency or unphysical results. One basic ‘pro’ for it is that the string theory does not exclude the possibility of the imaginary valued fields from the beginning. Let us consider a string field state in the string Fock space basis as

$$|\Psi\rangle = \int d^D p (\phi(p)|p\rangle + t_{\mu\nu}(p)\alpha_{-1}^\mu\tilde{\alpha}_{-1}^\nu|p\rangle + \dots), \quad (1.1)$$

where $\alpha_{-n}^\mu = (\alpha_n^\mu)^\dagger$, and so on, to ensure Hermiticity of the string coordinate field $X^\mu = X^{\mu\dagger}$. When we discuss excitations over time-independent vacua, we restrict the coefficients, $\phi(p)$, $t_{\mu\nu}(p)$, \dots , to be real. However, in principle, the coefficients can be complex without causing any logical inconsistency. There is no *a priori* reason to restrict the string field state to the one in real Fock space.

On the other hand, one might easily raise a naive ‘con’ too, against the imaginary valued fields. The situation gets more complicated if we couple the imaginary field with real valued charges. The coupling gives rise to an imaginary term in the Lagrangian in contrast with the real (though wrong signed) kinetic term. Our proposal is that we should interpret such a term in a semi-classical way as a signature of the instability of the vacuum. This is in the spirit of Schwinger’s original work [19] on the pair creation in a strong electric field. Here, the imaginary value of the effective potential has a definite physical interpretation. It induces the creation of spherical branes much like Schwinger’s process of pair creation.

This paper is one attempt in the direction and we will see it actually does not any serious harm to the story involving an unstable vacuum like de Sitter¹. It rather gives us a new insight about de Sitter space-time in the language of brane physics. Furthermore, the bubble solutions have a surprising cosmological application. The empirical evidences (the acceleration of the present universe and the dominant contribution from the matter component with the equation of state parameter $w \sim -1$ [2]) for the positive cosmological constant impose on us the problem of explaining

¹De Sitter space-time is classically stable in the sense that the cosmological constant persists its value with time. However, there could be some quantum instability like particle creation [20] or decaying to other de Sitter [21][22][23][24].

why the cosmological constant is so small but is yet non-vanishing. This ‘cosmological constant problem’ is notoriously difficult to solve. In this paper, we address this problem again in the context of string/M theories and find a surprisingly simple picture, which is generically quantum mechanical and also generically string theoretic. This is achieved by utilizing the created spherical branes as the factor which effectively lowers the cosmological constant of de Sitter space-time.

1.2 Detouring the No-go theorem in Supergravity

There are several ways to detour the no-go theorem [13]. For example, one can use some negative tension objects like O3-planes [25] or conceive of the compactification on some non-compact internal space like hyperbolic space [26]. In the same vein, quantum corrections and extended objects provide a controllable way to get de Sitter space-time while stabilizing all the moduli [27]. Although all these schemes were quite successful in getting to de Sitter space-time in the framework of string/M theories, we are still lost ironically in a vast landscape of de Sitter vacua [28].

In this paper, we suggest another way of detouring the no-go theorem; i.e., introducing imaginary fields, or equivalently real fields with wrong kinetic terms. One virtue of introducing the imaginary fields is that de Sitter space-time can be obtained in a very simple setup as an exact solution of Einstein equation. For example, let us take 4-dimensional Einstein-Maxwell system. The equations of motion (written in the orthonormal frame) taking the form,

$$R_{ab} = \frac{1}{2}F_{ac}F_b{}^c - \frac{1}{8}\eta_{ab}F_{cd}F^{cd}, \quad d*F^{(2)} = 0 \quad (1.2)$$

have the well-known Freund-Rubin type solution,

$$ds^2 = ds_{AdS}^2 + ds_{sphere}^2, \quad F^{(2)} = me^2 \wedge e^3, \quad (1.3)$$

where $e^2 \wedge e^3$ is the volume of the unit sphere. From the observation that the nontrivial components of Ricci tensor are $R_{00} = -R_{11} = R_{22} = R_{33} = m^2/4$, we are tempted to think of an imaginary valued field strength ($m^2 < 0$) so that the above solution get converted to the type

$$ds^2 = ds_{hyperbolic}^2 + ds_{dS}^2, \quad (1.4)$$

that is, the geometry factorized into two-dimensional hyperbolic space and two-dimensional de Sitter space-time.

A systematic way of making imaginary fields is the procedure of DWR. In contrast to the familiar single Wick rotation, (that is the analytic continuation to Euclidean space), DWR is a true symmetry at the action level. See Appendix A for a detailed proof. A typical form of DWR is

$$t = -i\xi, \quad x = i\psi, \quad (1.5)$$

which corresponds to the simultaneous Wick rotation of the temporal coordinate t and one of the spatial coordinates, x . Actually the Jacobian factor involved in this DWR is trivial and we need not define a new (DWR) version of the Lagrangian. Recall that in the conventional single Wick rotation procedure, we define Euclidean Lagrangian as

$$\mathcal{L}_E \left(q, \frac{dq}{dt_E} \right) \equiv -\mathcal{L} \left(q, i \frac{dq}{dt_E} \right), \quad (1.6)$$

that is minus of Minkowskian Lagrangian with the replacement $t = -it_E$.

Once we are given a set of solutions of the equations of motion, this discrete symmetry can be used to generate another set of solutions. This machinery works because the supergravity action is intact under DWR, therefore, the newly generated solutions solve the original equations of motion with appropriate boundary conditions.

1.3 Geometry near the Wall of Witten's Bubble

One typical example of thus made solution is the original Witten's bubble solution [29], obtained by double Wick rotating Schwarzschild black hole solution. Various aspects of bubble solutions have been considered in Refs. [30][31][32]. With string/M theories in mind, let us consider Schwarzschild black hole in general D -dimensions;

$$ds^2 = - \left(1 - \left(\frac{r_0}{r} \right)^{D-3} \right) dt^2 + \left(1 - \left(\frac{r_0}{r} \right)^{D-3} \right)^{-1} dr^2 + r^2 (d\theta^2 + \sin^2 \theta d\Omega_{D-3}^2). \quad (1.7)$$

Taking the following double Wick rotation,

$$t = -i\xi, \quad \theta = \frac{\pi}{2} + i\psi, \quad (1.8)$$

we obtain a bubble solution

$$ds^2 = \left(1 - \left(\frac{r_0}{r} \right)^{D-3} \right) d\xi^2 + \left(1 - \left(\frac{r_0}{r} \right)^{D-3} \right)^{-1} dr^2 + r^2 (-d\psi^2 + \cosh^2 \psi d\Omega_{D-3}^2). \quad (1.9)$$

The radial coordinate should be restricted as $r \geq r_0$, to prevent three temporal coordinates from appearing. Regularity at $r = r_0$ requires that the coordinate ξ be periodic;

$$\xi \sim \xi + \frac{4\pi r_0}{D-3}. \quad (1.10)$$

Asymptotically, the solution describes the standard Kaluza-Klein compactification. This is more transparent in Rindler coordinates,

$$\tau = r \sinh \psi, \quad \rho = r \cosh \psi, \quad (\tau^2 < \rho^2) \quad (1.11)$$

in which the asymptotic geometry becomes a circle times $(D - 1)$ -dimensional flat Minkowski space-time;

$$\begin{aligned} ds^2 &\simeq d\xi^2 + dr^2 + r^2 (-d\psi^2 + \cosh^2 \psi d\Omega_{D-3}^2) \\ &= d\xi^2 - d\tau^2 + d\rho^2 + \rho^2 d\Omega_{D-3}^2. \end{aligned} \quad (1.12)$$

The internal circle shrinks to zero size at $r = r_0$ and the geometry is not extended to the region $r < r_0$, thus it is called a bubble of nothing. The whole nowhere-singular solution describes a bubble of nothing with its wall accelerating in time ($\rho^2 = \tau^2 + r_0^2$). In this sense, the solution is also called as Kaluza-Klein bubble. Fig. 1 shows the snapshot of a bubble. In the asymptotic region, the geometry represents a flat Minkowski space-time Kaluza-Klein compactified on a circle of a period $\Delta\xi$.

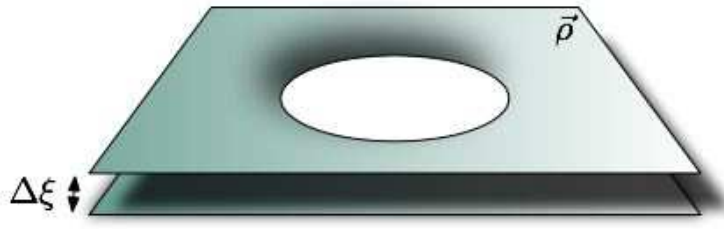


Figure 1: A Kaluza-Klein Bubble

Since the asymptotic isometry of the bubble solution is $U(1) \times SO(D - 2, 1)$, one is tempted to think of the ‘near-bubble’ geometry, where $(D - 2)$ -dimensional de Sitter space-time (with the isometry $SO(D - 2, 1)$) could be relevant. This looks plausible and the approximate geometry in the near-bubble region describes a disk and a $(D - 2)$ -dimensional de Sitter space-time;

$$ds^2 \simeq \frac{1}{r_0^{D-3}} \left(u^2 d\xi^2 + \frac{4r_0^2}{(D-3)^2} du^2 \right) + r_0^2 (-d\psi^2 + \cosh^2 \psi d\Omega_{D-3}^2). \quad (1.13)$$

Here, we introduced the near-bubble coordinate $u^2 = r^{D-3} - r_0^{D-3}$ and neglected the terms of order $\mathcal{O}(u^2/r_0^{D-3})$. However, we should not take this ‘factorization’ seriously because this approximate geometry does not solve the equation of motion exactly².

In this paper, we apply DWR to various D-brane and M-brane solutions well-known in string/M theories and get their bubble cousins. The non-extremal bubbles exhibit similar features as the Witten’s bubble; the solutions are restricted to the

²If there is some mechanism that makes the observer remain at fixed point of the radial coordinate u , then he will find himself in de Sitter space-time. This can be achieved by giving some angular momentum to the observer. In fact, this possibility was studied in Ref. [33] by considering the geodesic motions in a Kaluza-Klein bubble background.

outside of some fixed radial coordinate $r_0 > 0$, the asymptotic geometry describes Minkowski space-time compactified on a circle, and the bubble wall is accelerating in the asymptotic coordinates.

The extremal bubbles inherit most good features from their D-brane and M-brane counterparts. The geometry near the bubble wall, sharply factorized as de Sitter space-time and the hyperbolic space, is not just an approximate solution but an exact solution. The wall of the extremal bubbles follows a null line, nevertheless the near bubble solution preserves the full 32 supersymmetries.

However, those solutions are plagued by various imaginary valued fields therefore look ‘pathological’. This is the consequence of the DWR from the real valued fields of $\text{AdS}_p \times \text{S}^q$ backgrounds. The option one can choose at this point is either to abandon those solutions or to interpret their physical meaning. The strategy we will follow in this paper is the latter. We interpret the DWR procedure as a physical one; the de Sitter part including imaginary gauge fields as the instanton tunneling from S^4 to dS_{3+1} à la Coleman-de Luccia [36] or Hawking-Turok [37] in the spirit of Hartle-Hawking no-boundary proposal [38]. We would like to emphasize here that our solutions need not assume any false vacua as was done in Coleman-de Luccia instanton and are also in contrast with Hawking-Turok instanton in that they are geodesically complete without any singularity.

This semi-classical interpretation of the bubble solutions is not that unreasonable. Recall the motion of a particle in one dimension under a potential $V(x)$. For a given energy E of the particle, its motion under the potential barrier (the region where $E < V(x)$) is forbidden in the classical sense because there, its momentum $p = \sqrt{E - V(x)}$ becomes purely imaginary valued. We have no classical way to measure this imaginary momentum. However, the particle can actually be found under the potential barrier with a finite probability unless the barrier is infinitely high. At the quantum level, the measurement of the imaginary momentum is performed by measuring the probability of the particle to be under the barrier because WKB wave function of the particle is of the form $\psi(x) \sim e^{i \int^x p(x') dx'}$ with $p(x')$ imaginary valued [34]. The same physics of the tunneling process can be read via Euclidean method with purely real Euclidean momentum achieved by Wick rotation [35]. Though we obtained the bubble solutions solving the *classical* equations of motion, the way they obtained is semi-classical (double Wick rotation). As a result, we are cluttered by the imaginary values. The way we understand their physical meaning should also be semi-classical.

2. D-bubbles and M-bubbles

2.1 D/M-brane Configurations and their Bubble Cousins

Most well-known D/M-brane configurations have their bubble cousins. In this sec-

tion, we will study in detail the bubble solution obtained from a D3-brane solution. We will call it a D3-bubble. Bubble solutions can also be obtained from other well-known brane configurations, such as D1-D5. We can also study bubbles from M-branes, thus called M-bubbles. Details of these other bubble solutions can be found in the appendix B.

Let us start with a non-extremal D3-brane solution;

$$ds^2 = H_3^{-\frac{1}{2}}(r) (-f_3(r)dt^2 + d\vec{x}^2) + H_3^{\frac{1}{2}}(r) (f_3^{-1}(r)dr^2 + r^2 d\Omega_5^2),$$

$$H_3(r) = 1 + \frac{\mu_3^4 \sinh^2 \alpha_3}{r^4}, \quad f_3(r) = 1 - \frac{\mu_3^4}{r^4} \quad (2.1)$$

with the electric and the magnetic RR field strength as

$$\mathcal{F}_{(5)} = - * dH_m + d(H_e^{-1} - 1) \wedge dt \wedge dx_1 \wedge dx_2 \wedge dx_3$$

$$= 4\mu_3^4 \sinh \alpha_3 \cosh \alpha_3 (d\Omega_5 + r^{-5} H_3^{-2} dt \wedge dx_1 \wedge dx_2 \wedge dx_3 \wedge dr),$$

$$H_m = 1 + \frac{\mu_3^4 \sinh \alpha_3 \cosh \alpha_3}{r^4}, \quad H_e^{-1} - 1 = - \frac{\mu_3^4 \sinh \alpha_3 \cosh \alpha_3}{r^4 + \mu_3^4 \sinh^2 \alpha_3}. \quad (2.2)$$

Here, Hodge star $*$ is with respect to the 6-dimensional *flat* space transverse to the brane world-volume. We followed the notations for the harmonic functions from Ref. [39].

The bubble geometry is obtained à la Witten (1.8) [29]. Double Wick rotations along the temporal direction and one of the spherical direction lead us to

$$ds^2 = H_3^{-\frac{1}{2}}(r) (f_3(r)d\xi^2 + d\vec{x}^2) + H_3^{\frac{1}{2}}(r) (f_3^{-1}(r)dr^2 + r^2 (\cosh^2 \psi d\Omega_4^2 - d\psi^2)). \quad (2.3)$$

The fact that RR field strength is involved in the solution is basically in contrast with Witten's bubble (1.9). It results in the 'unwanted' imaginary value of the field;

$$\mathcal{F}_{(5)} = 4i\mu_3^4 \sinh \alpha_3 \cosh \alpha_3 (\cosh^4 \psi d\Omega_4 \wedge d\psi - r^{-5} H_3^{-2} d\xi \wedge dx_1 \wedge dx_2 \wedge dx_3 \wedge dr). \quad (2.4)$$

However, as was mentioned earlier, we will interpret this imaginary value of the solution as some quantum process like instanton.

2.2 Near-Bubble Geometries and de Sitter space-time

Here, we will see that near bubble geometries contain de Sitter space-time. In the near-bubble coordinate ($u^2 = r^4 - \mu_3^4$, $u^2 \ll \mu_3^4$), the harmonic functions are well approximated by

$$f_3(u) = \frac{u^2}{u^2 + \mu_3^4} \simeq \frac{u^2}{\mu_3^4}$$

$$H_3(u) = \frac{u^2 + \mu_3^4 \cosh^2 \alpha_3}{u^2 + \mu_3^4} \simeq \cosh^2 \alpha_3$$

$$H_m(u) = \frac{u^2 + \mu_3^4 (1 + \sinh \alpha_3 \cosh \alpha_3)}{u^2 + \mu_3^4} \simeq 1 + \sinh \alpha_3 \cosh \alpha_3. \quad (2.5)$$

As a consequence, the metric takes the form;

$$\begin{aligned}
ds^2 &\simeq \frac{\cosh \alpha_3}{4\mu_3^2} \left(du^2 + \frac{4u^2}{\mu_3^2 \cosh^2 \alpha_3} d\xi^2 \right) + \cosh^{-1} \alpha_3 \sum_{i=1}^3 dx_i^2 \\
&\quad + \mu_3^2 \cosh \alpha_3 (-d\psi^2 + \cosh^2 \psi d\Omega_4^2), \\
\mathcal{F}_{(5)} &\simeq 4i\mu_3^4 \sinh \alpha_3 \cosh \alpha_3 (\cosh^4 \psi d\Omega_4 \wedge d\psi \\
&\quad - \frac{u}{2(\mu_3^4 \cosh^2 \alpha_3)^2} d\xi \wedge dx_1 \wedge dx_2 \wedge dx_3 \wedge du).
\end{aligned} \tag{2.6}$$

In order for the geometry to be geodesically complete, the compact direction ($\xi \sim \xi + 2\pi\hat{R}$) should have a periodicity $\hat{R} = (\mu_3 \cosh \alpha_3)/2$. The geometry then becomes factorized into $D_2 \times \mathbf{R}^3 \times dS_{4+1}$, where D_2 stands for a two-dimensional disk and the 5-dimensional de Sitter space-time dS_{4+1} has the cosmological constant $\Lambda_{4+1} = 6/(\mu_3^2 \cosh \alpha_3)$.

2.3 Exact Near-Bubble Solutions: Extremal Cases

Though the near-bubble geometry involves de Sitter space-time, it should be understood only in the approximate sense. Meanwhile in the extremal case, one can expect an exact factorization of the near bubble geometry as the DWR version of the $AdS_{4+1} \times S^5$.

The extremal case can be obtained by limiting $\mu_3 \rightarrow 0$ and $\alpha_3 \rightarrow \infty$ with $Q_3 = \mu_3^4 \sinh \alpha_3 \cosh \alpha_3$ kept finite. The resulting near bubble configuration is

$$\begin{aligned}
ds^2 &= \sqrt{Q_3} \left(\frac{1}{r^2} dr^2 + \frac{r^2}{Q_3} \left(d\xi^2 + \sum_{i=1}^3 dx_i^2 \right) \right) + \sqrt{Q_3} (-d\psi^2 + \cosh^2 \psi d\Omega_4^2), \\
\mathcal{F}_{(5)} &= 4iQ_3 \left(\cosh^4 \psi d\psi \wedge d\Omega_4 - \frac{r^3}{Q_3^2} d\xi \wedge dx_1 \wedge dx_2 \wedge dx_3 \wedge dr \right).
\end{aligned} \tag{2.7}$$

The near-bubble geometry ($r^4 \ll Q_3$) clearly includes 5-dimensional de Sitter part (with the cosmological constant $\Lambda_{4+1} = 6/\sqrt{Q_3}$). The first part in the above geometry actually describes a 5-dimensional hyperbolic space, whose Ricci tensor components are

$$R_{rr} = -\frac{4}{\sqrt{Q_3}} g_{rr}, \quad R_{\xi\xi} = -\frac{4}{\sqrt{Q_3}} g_{\xi\xi}, \quad R_{ij} = -\frac{4}{\sqrt{Q_3}} g_{ij} \quad (i = 1, 2, 3). \tag{2.8}$$

The curvature scalar is given by $R = -20/\sqrt{Q_3}$.

The geometry is geodesically complete as far as $r \geq 0$ and there is no reason to make ξ compact, being in contrast with the non-extremal case. However, one can take the direction ξ compact to make a null bubble (a ‘bubble’ in that the size of Kaluza-Klein compact direction vanishes at $r = 0$ and ‘null’ in that its wall follows a null line). The causal structures of the bubbles are drawn in Fig. 2, where all the

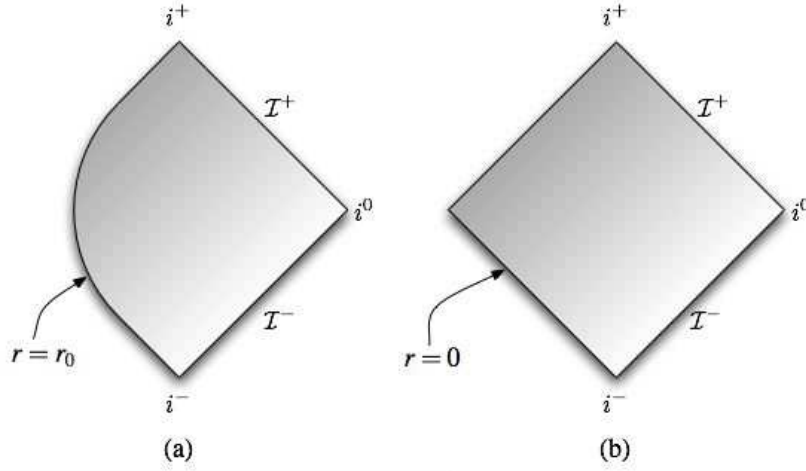


Figure 2: Penrose diagrams for (a) the non-extremal bubble, and (b) the extremal bubble.

directions other than the temporal direction ψ and the radial direction r have been suppressed. The space and time are restricted only to the shaded region, outside of which there is ‘nothing’.

We restrict our interest to the extremal case and try to identify the source that generates the bubble geometry. It carries the electric and magnetic RR flux, though imaginary. With the notion that its AdS cousin is the D3-branes with their world-volume directions (t, x_1, x_2, x_3) , it is natural to think of some 4-dimensional object that extend to the directions (ξ, x_1, x_2, x_3) . It is instanton-like in the sense that it is localized at the center in the transverse directions including the time ψ .

Integrating the 5-form field strength over the hyperbolic space that is transverse to de Sitter space-time, we obtain the magnetic flux

$$\begin{aligned}
 \int_{H_5} \mathcal{F}_{(5)} &= -4iQ_3 \int_{H_5} r^{-5} H_3^{-2} d\xi \wedge dx_1 \wedge dx_2 \wedge dx_3 \wedge dr \\
 &= -4iQ_3 \text{Vol}_4 \int_0^\infty dr \frac{r^3}{(r^4 + Q_3)^2} \\
 &= -i \text{Vol}_4
 \end{aligned} \tag{2.9}$$

and the electric flux,

$$\begin{aligned}
 \int_{H_5} * \mathcal{F}_{(5)} &= 4iQ_3 \int_{H_5} * (\cosh^4 \psi d\psi \wedge d\Omega_4) \\
 &= 4iQ_3 \int_{H_5} r^{-5} H_3^{-2} d\xi \wedge dx_1 \wedge dx_2 \wedge dx_3 \wedge dr \\
 &= i \text{Vol}_4,
 \end{aligned} \tag{2.10}$$

where Vol_4 is the coordinate volume of the anti-selfdual ‘instanton’. It is very interesting to see that both the electric and magnetic flux density are independent of

the number Q_3 of D3-brane cousins. This is a universal feature common to most D/M-bubble configurations. In later part of this paper, we use this feature as one important clue to give the answer to the cosmological constant problem.

One can take DWR on other D/M-brane configurations to get their corresponding D/M-bubble solutions. Since the procedure is straightforward, we defer the details to the appendix and only summarize the results in Table 1, where we tabulated the geometrical properties of the various D/M-bubbles. The second and the third columns summarize the near-bubble geometries of various non-extremal and extremal D/M-bubbles. In the non-extremal cases, the above factorized geometries are to be understood only in the approximate sense. The cosmological constants Λ 's are the same both in the extremal and in the non-extremal cases (the 4-th column). The electric and the magnetic flux densities over the hyperbolic space are mostly fixed to $\pm i$ being irrespective of the number of source branes. The electric flux density of D1-D5-bubble is one exception and its value approaches to i only as $Q_1 \rightarrow Q_5$.

bubble type	non-extremal	extremal	Λ of dS	electric	magnetic
D3	$D_2 \times \mathbf{R}^3 \times dS_{4+1}$	$H^5 \times dS_{4+1}$	$6/\sqrt{Q_3}$	i	$-i$
D1-D5	$D_2 \times \mathbf{R}^5 \times dS_{2+1}$	$H^7 \times dS_{2+1}$	$1/\sqrt{Q_1 Q_5}$	$i \frac{\ln \frac{Q_1}{Q_5}}{(\frac{Q_1}{Q_5} - 1)}$	$-i$
M2	$D_2 \times \mathbf{R}^2 \times dS_{6+1}$	$H^4 \times dS_{6+1}$	$15/\sqrt[3]{Q_T}$	none	i
M5	$D_2 \times \mathbf{R}^5 \times dS_{3+1}$	$H^7 \times dS_{3+1}$	$3/\sqrt[3]{Q_F^2}$	$-i$	none

Table 1: Various D/M-bubbles

With the temporal coordinate ψ being transverse to the ‘world volume’ directions, the bubble solutions could have some relation with Hull’s Euclidean branes (E-branes) [14] or Gutperl and Strominger’s spacelike branes (S-branes) [40]. (For more recent issues about E-branes or S-branes, see Ref. [41].) Indeed D3-bubble solutions correspond to E4-brane solutions in type IIB theory. One can see this explicitly by adopting Rindler coordinates (1.11);

$$\tau = r \sinh \psi, \quad \rho = r \cosh \psi. \quad (2.11)$$

The D3-bubble solutions in these coordinates become

$$ds^2 = H_3^{-\frac{1}{2}}(\tau, \rho) (d\xi^2 + d\bar{x}^2) + H_3^{\frac{1}{2}}(\tau, \rho) (-d\tau^2 + d\rho^2 + \rho^2 d\Omega_4^2), \quad (2.12)$$

where the harmonic function is given by

$$H_3(r(\tau, \rho)) = 1 + \frac{Q_3}{r^4} = 1 + \frac{Q_3}{(\rho^2 - \tau^2)^2}. \quad (2.13)$$

RR field strength becomes

$$\begin{aligned}\mathcal{F}_{(5)} = 4iQ_3 & \left(\frac{\rho^4}{(\rho^2 - \tau^2)^3} d\Omega_4 \wedge (\rho d\tau - \tau d\rho) \right. \\ & \left. - \frac{1}{(\rho^2 - \tau^2)^3 H_3^2} d\xi \wedge dx_1 \wedge dx_2 \wedge dx_3 \wedge (\rho d\rho - \tau d\tau) \right). \quad (2.14)\end{aligned}$$

Hence the whole results suggest the equivalence between DWR and Hull's time-like T-duality. More specifically to say, DWR is the combination of T-dualities along one of the transverse directions and along the temporal direction;

$$\text{DWR} = \mathbf{T}_t \cdot \mathbf{T}_\perp. \quad (2.15)$$

In Hull's solution, RR field strength is real valued but it was instead embedded into a $*$ -theory with unusual 'wrong signed' kinetic terms for RR fields. One can recast the above solutions to those of $*$ -theory by redefining RR fields as $\mathcal{F}_{(5)} \equiv iF_{(5)}$. We would like to emphasize that one virtue of DWR over the timelike T-duality is that the former can be applied to the solutions of M-theory, where T-duality is ambiguous.

3. Multi-Bubbles : Swiss Cheese Universe

3.1 Maximal Supersymmetries near the Walls of Extremal Bubbles

In order to make sense of multi-bubble solutions, we have to check whether there is any supersymmetry preserved by the bubble background. This issue is very confusing. On the one hand, there is a definite argument against the supersymmetry in de Sitter space-time. The argument is based on the fact that there is no positive conserved energy in de Sitter space-time. Roughly speaking, assuming any supersymmetry contradicts with this fact. See Ref. [10] for details. On the other hand, we know the D/M-brane partners of the bubbles discussed in this paper preserve supersymmetries. Since DWR does not change the numbers of positive or negative signature in the metric, the spinor structure will be untouched.

Although extremal bubbles are time-dependent solutions³ and have de Sitter regions, there are supersymmetries preserved. In fact, all of 32 supersymmetries are preserved in the near-bubble regime of most D/M-bubbles except D1-D5-bubble case where 16 supersymmetries are preserved. In the following, to be more specific, we will focus on M5-bubble case and obtain Killing spinors explicitly. The secret of this surprising result is mainly due to the imaginary valuedness of higher form fields.

³Strictly speaking, time-dependence does not necessarily imply supersymmetry breaking. For some examples of time-dependent but supersymmetric configuration of D-branes, see Refs. [42][43][44].

With all the details concerning vielbein components and spin connection components in appendix C, the Killing spinor equations in eleven dimensional supergravity read as

$$0 = \delta\psi_\mu = D_\mu\epsilon + \frac{1}{288}(\Gamma_\mu^{\nu\rho\sigma\kappa} - 8\delta_\mu^\nu\Gamma^{\rho\sigma\kappa})\epsilon\mathcal{F}_{\nu\rho\sigma\kappa}, \quad (3.1)$$

where $\mathcal{F}_{(4)}$ denotes 4-form field strength. The spinor ϵ is a 32-component Majorana and

$$\Gamma^{a_1 a_2 \dots a_n} = \frac{1}{n!} \left(\Gamma^{a_1} \Gamma^{a_2} \dots \Gamma^{a_n} + \sum \text{(anti-symmetric combinations)} \right). \quad (3.2)$$

In the above equations, we used 11-dimensional gamma matrices satisfying

$$\{\Gamma^a, \Gamma^b\} = 2\eta^{ab}. \quad (3.3)$$

For the purpose of solving Killing spinor equations, it is convenient to work in the orthonormal frame, where 4-form field strength is expanded in the case of S^4 or dS_{3+1} as

$$\begin{aligned} \mathcal{F} &= -3Q \sin^2 \chi_3 d\Omega \wedge d\chi_3 = -3Q^{-\frac{1}{3}} e^7 \wedge e^8 \wedge e^9 \wedge e^\sharp \\ &= -3iQ \sinh^2 \psi d\Omega \wedge d\psi = -3iQ^{-\frac{1}{3}} \bar{e}^7 \wedge \bar{e}^8 \wedge \bar{e}^9 \wedge \bar{e}^\sharp. \end{aligned} \quad (3.4)$$

In order to denote the cases of $AdS_{6+1} \times S^4$ and $H^7 \times dS_{3+1}$ collectively, we represent the components $\eta^{00} \equiv \eta$ and $\eta^{\sharp\sharp} \equiv \kappa^2$ as

$$\begin{aligned} \eta &= -1 & \kappa &= 1 & (AdS_{6+1} \times S^4), \\ \eta &= 1 & \kappa &= i & (H^7 \times dS_{3+1}). \end{aligned} \quad (3.5)$$

The Killing spinor equations are then recast in the orthonormal frame as

$$\begin{aligned} 0 &= \partial_\mu\epsilon + \frac{1}{4}\omega_{ab\mu}\Gamma^{ab}\epsilon + \frac{1}{2^5 \cdot 3^2} (e^a_\mu\Gamma_a^{bcde} - 8e^b_\mu\Gamma^{cde})\epsilon\mathcal{F}_{bcde} \\ &\equiv \partial_\mu\epsilon + \frac{1}{2}\Omega_\mu\epsilon. \end{aligned} \quad (3.6)$$

The explicit forms of the matrices Ω_μ are listed in Appendix C.4. Despite of their complicated expression, most components Ω_μ are squared to -1 except $\Omega_t^2 = \eta$, $\Omega_\lambda^2 = \Omega_\psi^2 = 1$. One more property relevant in the computation of the Killing spinors is that Ω_μ 's of AdS_{6+1}/H^7 part and those of S^4/dS_{3+1} part mutually commute.

The final form of the Killing spinors satisfying all the above equations is

$$\epsilon = \Omega_{AdS/H} \cdot \Omega_{S/dS} \cdot \epsilon_0, \quad (3.7)$$

where

$$\begin{aligned} \Omega_{AdS/H} &= e^{\frac{\theta_4}{2}\Gamma^{16}} e^{-\frac{\theta_3}{2}\Gamma^{56}} e^{-\frac{\theta_2}{2}\Gamma^{45}} e^{-\frac{\theta_1}{2}\Gamma^{34}} e^{-\frac{\varphi}{2}\Gamma^{23}} e^{\frac{\kappa\lambda}{2}\Gamma^{1789\sharp}} e^{\frac{\kappa\eta t}{2}\Gamma^{0789\sharp}} \\ \Omega_{S/dS} &= \begin{cases} e^{\frac{\chi_3}{2}\Gamma^{789}} e^{-\frac{\chi_2}{2}\Gamma^{9\sharp}} e^{-\frac{\chi_1}{2}\Gamma^{89}} e^{-\frac{\phi}{2}\Gamma^{78}} & (S^4) \\ e^{\frac{1}{2}(i\psi+\frac{\pi}{2})\Gamma^{789}} e^{-\frac{i\chi_2}{2}\Gamma^{9\sharp}} e^{-\frac{\chi_1}{2}\Gamma^{89}} e^{-\frac{\phi}{2}\Gamma^{78}} & (dS_{3+1}) \end{cases} \end{aligned} \quad (3.8)$$

and ϵ_0 is an arbitrary 32-component constant Majorana spinor. Hence the whole supersymmetries are preserved for both $\text{AdS}_{6+1} \times S^4$ and $H^7 \times dS_{3+1}$ cases.

The secret of this supersymmetric de Sitter space-time lies in the imaginary field strength which enables the nice property of $(\Omega_\mu)^2 = \pm 1$, that is, they become coordinate independent once squared. Lastly, we note one very interesting point about the periodicity of Killing spinors. Although the coordinate t that was the temporal coordinate in AdS space-time, should be replaced by ξ in the hyperbolic space and it need not to be quantized because

$$(\kappa \eta \Gamma^{0789})^2 = \eta = 1. \quad (3.9)$$

On the contrary, the temporal coordinate t should be quantized as $t \sim t + 2\pi n$ ($n \in \mathbf{Z}$) in AdS case, where we use the universal covering to avoid this unwanted feature.

3.2 Null Geodesic Lines in the Bubble Geometry

In a realistic cosmological situation, one can expect that actually there are multiple bubbles. In case of two bubbles, both of which are expanding, the collision of bubbles might lead to the formation of singularity [45]. This sounds that the inhabitants near the bubble walls are destined to have a doomsday.

However, if we live near the bubble wall, we will never witness the singularity formation. This means we cannot observe the bubbles swallow up us. For the purpose of seeing this, it is instructive to consider the null geodesic lines in the near-bubble coordinates (ψ, r) and in the asymptotic Rindler coordinates (τ, ρ) respectively. In the former coordinates, the null geodesic in the bubble background is determined by the equation

$$0 = H(r) (dr^2 - r^2 d\psi^2). \quad (3.10)$$

Here, $H(r)$ is a certain harmonic function specified by the brane type. In the near-bubble coordinates, the null geodesic lines passing through the point (ψ_i, r_i) are represented as

$$\psi = \pm \ln \frac{r}{r_i} + \psi_i, \quad (3.11)$$

where the sign $+/ -$ corresponds to the outgoing/ingoing null rays respectively. One thing to note is that it takes infinite coordinate time ($\psi \rightarrow \infty$) for the null rays to reach or to come out of the bubble wall.

The situation viewed from the asymptotic observer is different. In his coordinates $(\tau, \rho) = (r \sinh \psi, r \cosh \psi)$, the null geodesic lines are determined by

$$0 = H(\tau, \rho) (d\rho^2 - d\tau^2), \quad (3.12)$$

and it takes finite coordinate time ($\tau < \infty$) for the null rays to reach or to come out of the bubble wall. This property is illustrated in Fig. 3.

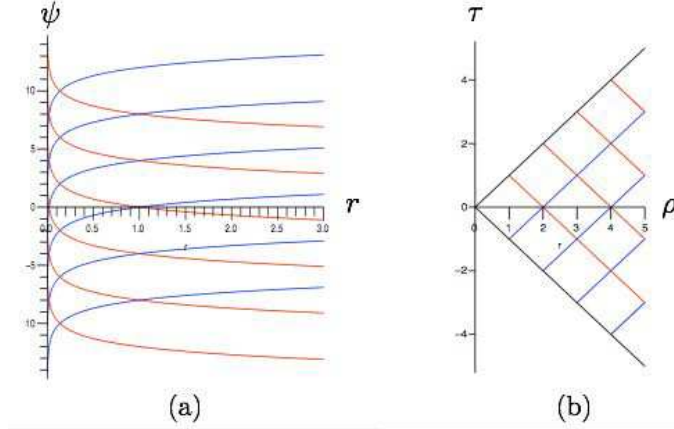


Figure 3: Null geodesic lines (a) in the near-bubble coordinates (ψ, r) and (b) in the asymptotic Rindler coordinates (τ, ρ) . The red lines are incoming and the blue lines are outgoing.

Each intersection of the ingoing (red) null lines and the outgoing (blue) null lines composes a null cone. Especially in the near-bubble coordinates (ψ, r) , the null cones get pinched off and nothing can reach the wall in a finite coordinate time ψ . Actually this is related to the fact that ψ itself is a good affine parameter and the bubble geometry is geodesically complete.

3.3 Bubble Landscape - Swiss Cheese Universe

Starting from various multi-brane solutions, one can obtain their corresponding bubble cousins via the double Wick rotation. For simplicity, we focus on the extremal M5-brane case that results in various 4-dimensional de Sitter space-times.

Generalizing the harmonic function to the multi-centered one, we get the multi-bubble solution;

$$H_F \Rightarrow 1 + \sum_a \frac{Q_a}{|\vec{r} - \vec{r}_a|^3}, \quad (3.13)$$

according to which 4-form field strength becomes

$$\mathcal{F}_{(4)} = -3i \sum_a \frac{Q_a r^3 \vec{r} \cdot (\vec{r} - \vec{r}_a)}{|\vec{r} - \vec{r}_a|^5} \cosh^3 \psi d\psi \wedge d\Omega_3. \quad (3.14)$$

If there is some region close to all the bubbles ($|\vec{r} - \vec{r}_a|^3 \ll Q_a$), there, the metric looks like

$$ds^2 = \left(\sum_a \frac{Q_a}{|\vec{r} - \vec{r}_a|^3} \right)^{-\frac{1}{3}} \left(d\xi^2 + \sum_{i=1}^5 dx_i^2 \right) + \left(\sum_a \frac{Q_a}{|\vec{r} - \vec{r}_a|^3} \right)^{\frac{2}{3}} (dr^2 - r^2 d\psi^2 + r^2 \cosh^2 \psi d\Omega_3^2). \quad (3.15)$$

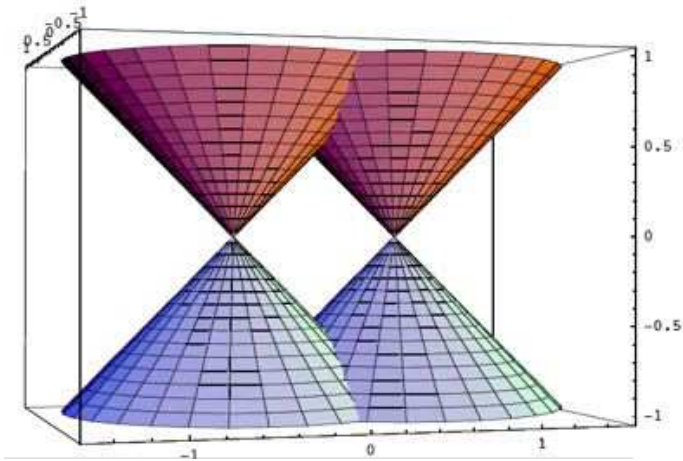


Figure 4: Two colliding bubbles drawn in the asymptotic coordinates $(\tau, \vec{\rho})$. The cones bound the space-time outside, while there is ‘nothing’ inside.

Fig. 4 exhibits two colliding bubbles drawn in the asymptotic coordinates $(\tau, \vec{\rho})$. The geometry is defined only outside of both null cones. Near two bubbles, the geometry is almost factorized into de Sitter and the hyperbolic space but the effective cosmological constant varies from point to point. Some aspects of colliding Witten’s bubble solutions were considered in Ref. [45].

In order to see the resulting de Sitter space-time explicitly, let us be specific to the case of two-bubbles with equal charge just for simplicity. The harmonic function of two-bubbles at $\vec{r}_{1,2} = (\pm a, 0, 0, 0)$ will be

$$H_F = 1 + \frac{Q}{(r^2 \sin^2 \theta_1 + (r \cos \theta_1 - a)^2)^{\frac{3}{2}}} + \frac{Q}{(r^2 \sin^2 \theta_1 + (r \cos \theta_1 + a)^2)^{\frac{3}{2}}} \quad (3.16)$$

In the region close to two bubbles, where the last two terms of the harmonic function become dominant over the constant ‘1’, but with $a/r \ll 1$, that is in the region $a \ll r \ll (2Q)^{\frac{1}{3}}$, the geometry is almost factorized into $dS_{3+1} \times H^7$;

$$ds^2 = (2Q)^{-\frac{1}{3}} r \left(1 - \frac{1}{2} (5 \cos^2 \theta_1 - 1) \frac{a^2}{r^2} + \mathcal{O} \left(\frac{a^4}{r^4} \right) \right) \left(d\xi^2 + \sum_{i=1}^5 dx_i^2 \right) \quad (3.17)$$

$$+ \frac{(2Q)^{\frac{2}{3}}}{r^2} \left(1 + (5 \cos^2 \theta_1 - 1) \frac{a^2}{r^2} + \mathcal{O} \left(\frac{a^4}{r^4} \right) \right) (dr^2 - r^2 d\psi^2 + r^2 \cosh^2 \psi d\Omega_3^2).$$

The effective cosmological constant in the region is $\Lambda \sim 3/(2Q)^{\frac{2}{3}}$. If we restrict to the region very close to one of those two bubbles so that only one of the harmonic terms is relevant, then the corresponding cosmological constant will be increased to $3/Q^{\frac{2}{3}}$. This could be a stringy realization of position-dependent cosmological constant. Such a concept is not new; quintessence [46] and k-essence [47] have such a feature. However we would like to emphasize that we need not introduce extra scalar fields to account for that.

Though the multi-bubble geometry looks static in the above near-bubble coordinates, the bubbles are expanding in the light speed and collide with one another in the asymptotic Rindler coordinates $(\tau, \rho) = (r \sinh \psi, r \cosh \psi)$, in which the single bubble geometry is described as

$$ds^2 = H_F^{-\frac{1}{3}} \left(d\xi^2 + \sum_{i=1}^5 dx_i^2 \right) + H_F^{\frac{2}{3}} (-d\tau^2 + d\rho^2 + \rho^2 d\Omega_3^2). \quad (3.18)$$

Here, the harmonic function H_F is

$$H_F = 1 + \frac{Q}{(-\tau^2 + \rho^2)^{\frac{3}{2}}} = 1 + \frac{Q}{(-\tau^2 + \sum_{i=1}^4 y_i^2)^{\frac{3}{2}}}. \quad (3.19)$$

In the last equality, we used the rectangular coordinates y_i ($i = 1, \dots, 4$) in which the second part of the metric (3.18) is written as $H_F^{2/3}(-d\tau^2 + \sum_{i=1}^4 dy_i^2)$. We note here that the geometry is restricted to the region exterior to the null cone $\rho^2 = \tau^2$ because $\rho^2 - \tau^2 = r^2 > 0$. Especially if ξ is compact, the asymptotic region where $H_F \simeq 1$, is a flat $(9+1)$ -dimensional space-time compactified on a circle. At $r^2 = \rho^2 - \tau^2 = 0$, the compact dimension pinches off because any finite period of ξ is suppressed by the factor $H_F^{-1/3}$. Therefore the whole geometry exterior to the null cone is geodesically complete space-time without any singularity and describes the null shock wave of a ‘bubble of nothing’ collapsing and re-expanding.

The harmonic function corresponding to the multi-bubble solution will be

$$H_F \Rightarrow 1 + \sum_a \frac{Q_a}{(-(\tau - \tau_a)^2 + (\vec{y} - \vec{y}_a)^2)^{\frac{3}{2}}}. \quad (3.20)$$

The bubbles are located at (τ_a, \vec{y}_a) and are separated from one another by the space-like distances because $-\Delta\tau^2 + \Delta\vec{y}^2 = \Delta\vec{r}^2 > 0$. In the same vein, the geometry is restricted to the region exterior to all the bubbles.

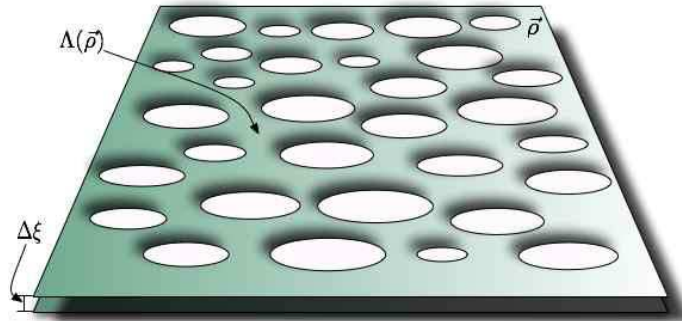


Figure 5: Swiss-cheese-like geometry of a multi-bubble solution

Fig. 5 visualizes Swiss-cheese-like geometry of a multi-bubble solution. The bubbles are expanding at the light speed but no observer can see them swallow up

the whole space-time completely because all the observers will be left, being squeezed by the expanding bubbles, to the near-bubble region where time coordinate ψ is the affine parameter. Depending on the position in $\vec{\rho} \in \mathbf{R}^4$, the effective cosmological constant varies. Notice that there is a ‘Universe’ corresponding to each bubble and the multi-bubble background gives rise to the multi-verse picture. Some of the earlier ideas of multi-verse can be found, for example in Refs. [48][49]. Varying cosmological constant in the multi-verse is reminiscent of more recent idea of landscape [28].

4. Semi-classical Instability of de Sitter Space-times

4.1 The Creation of Spherical M2 Branes in M5-Bubble Background

The only price we have to pay for de Sitter solution in string/M theories was to allow the imaginary field strengths. In this section, we interpret this disturbing situation as one mechanism to temper the acceleration of the universe so that it lead to de Sitter space-time with almost, but not exactly vanishing cosmological constant like our present universe.

Before going into details, we note that the imaginary valued term in the quantum effective action indicates the instability of the vacuum [19]. This statement is valid even in the classical action. Recall that Schrödinger equation tells us that the imaginary potential term in the classical action leads to the source term in the continuity equation for the probability density and the probability flux density;

$$\begin{aligned} \frac{\partial}{\partial t} \rho(t, \vec{x}) + \nabla \cdot \vec{j} &= \frac{\partial}{\partial t} (\psi^*(t, \vec{x}) \psi(t, \vec{x})) + \nabla \cdot \left(\frac{\hbar}{m} \text{Im}(\psi^*(t, \vec{x}) \nabla \psi(t, \vec{x})) \right) \\ &= \frac{i}{\hbar} (V^*(\vec{x}) - V(\vec{x})) (\psi^*(t, \vec{x}) \psi(t, \vec{x})). \end{aligned} \quad (4.1)$$

Therefore the imaginary potential term in the *classical action* indicates the violation of the unitarity, in other words, the creation of probability, at the *quantum* level.

Though the supergravity action is invariant under DWR, therefore real valued for the specific bubble solutions discussed so far, there might be some imaginary valued term being involved when probe D/M-branes are on their ways in these backgrounds. If so, we have to worry about the instability of the backgrounds themselves. Indeed the backgrounds are unstable at the semi-classical level. To be more explicit, let us focus on the M5-bubble geometry, in which de Sitter part of the near-bubble metric is given by

$$ds_{3+1}^2 = Q^{\frac{2}{3}} (-d\psi^2 + \cosh^2 \psi (d\theta_1^2 + \sin^2 \theta_1 d\Omega_2^2)). \quad (4.2)$$

Let us assume a spherical membrane composed of multi-sheets at constant θ_1 , then it will couple to the imaginary 4-form field strength via

$$q \int C^{(3)} = q \int d\psi \cosh^3 \psi \wedge A^{(2)}, \quad (4.3)$$

where q is proportional to the number of the membrane sheets and its sign denotes the orientation of the membrane. The part $A^{(2)}$ composing the gauge connection has been introduced just for the notational convenience and is given by

$$A^{(2)} = \begin{cases} A_N^{(2)} = \frac{-3iQ}{2} \left(\frac{\sin 2\theta_1}{2} - \theta_1 \right) d\Omega_2 & (0 \leq \theta_1 < \pi), \\ A_S^{(2)} = \frac{-3iQ}{2} \left(\frac{\sin 2\theta_1}{2} - \theta_1 + \pi \right) d\Omega_2 & (0 < \theta_1 \leq \pi). \end{cases} \quad (4.4)$$

In order to make the gauge fields well-defined, we introduced different gauges field in the northern and the southern hemi-3-sphere. In spherical coordinates, every connection form field concerning the azimuthal direction is ill-defined at the poles unless its value vanishes there. This is in analogy with the case of Dirac monopole. The difference of those two gauge fields, at any point of constant θ_1 different from 0 or π , is an exact form involving

$$A_N^{(2)} - A_S^{(2)} = \frac{3\pi i Q}{2} d\Omega_2. \quad (4.5)$$

The spherical membrane embedded into the spatial section S^3 of de Sitter bounds two 3-balls. The field strengths inside both balls induce different gauge fields via Stokes theorem on their common boundary, the spherical membrane. In Fig. 6, we draw the relative values of the gauge fields $A_N^{(2)}$ (from the north 3-ball) and $A_S^{(2)}$ (from the south 3-ball).

Despite of the analogy with Dirac monopole, there are some differences between them. First, the imaginary interaction term causes some instability of the vacuum (pure de Sitter space-time). When the above interaction term gets exponentiated with extra quantum factor i/\hbar , it gives a decaying factor, rather than the conventional oscillatory phase. This could be understood as the instability in the vacuum-to-vacuum transition in the semi-classical sense. Second, the instability depends on whether the spherical membrane couples to the connection involving $A_N^{(2)}$ or $A_S^{(2)}$. Recall that the gauge choice does not matter in the monopole case due to Dirac quantization condition of the electric and magnetic charges. In the case at hand, the electric flux over the whole de Sitter space-time is not a conserved quantity⁴ and what is worse is that such a condition as Dirac quantization is not helpful in removing the gauge ambiguity.

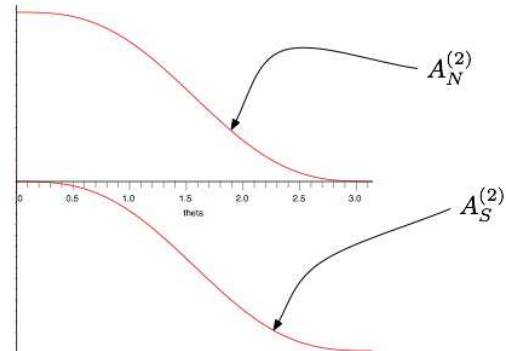


Figure 6: The relative values of the gauge fields $A_N^{(2)}$ (from the north 3-ball) and $A_S^{(2)}$ (from the south 3-ball)

The conserved electric flux is over the transverse 7-hyperboloid.

⁴The conserved electric flux is over the transverse 7-hyperboloid.

In order to fix up this ambiguity, we have to find a gauge invariant interaction of the spherical membrane with the imaginary background field. As was alluded earlier, the spherical membrane being embedded into the spatial 3-sphere, bounds two regions of 3-balls. It is reasonable to think that the spherical membrane couples to the background gauge fields from both 3-balls in a gauge invariant way:

$$\begin{aligned} q \int d\psi \cosh^3 \psi \int_{S^2} \left(A_N^{(2)} - A_S^{(2)} \right) &= q \int d\psi \cosh^3 \psi \int_{S^2} \frac{3\pi i Q}{2} d\Omega_2 \\ &= 6\pi^2 i q Q \int d\psi \cosh^3 \psi. \end{aligned} \quad (4.6)$$

The relative different signs of the gauge potentials in the first expression are due to different orientations of the north and the south 3-balls which the spherical membrane bounds.

This imaginary interaction term represents the instability of pure de Sitter vacuum against the creation of spherical membranes over its 3-spherical space. This is similar to Schwinger pair production procedure of charged particles in a strong electric field. Recall that the one-loop diagram of charged particles in the background of the strong electric field results in the pure imaginary term in the effective action, which implies the instability of the corresponding vacuum and signals the pair creation of the charged particles [19]. In the above, we get a pure imaginary term in the interaction of a spherical membrane (the composite of q M2-branes and q anti-M2-branes) with de Sitter background. When $qQ > 0$, one can interpret this term in the semi-classical sense as the instability of the de Sitter vacuum and signals the creation of spherical membranes with the rate,

$$2 \operatorname{Im} \mathcal{L} = 6\pi^2 q Q \cosh^3 \psi, \quad (4.7)$$

per unit coordinate volume and per unit coordinate time.

In all, M5-bubble de Sitter vacua is unstable against the creation of spherical membranes (See Fig. 7(a)). The spherical membrane with the opposite orientation (i.e., opposite sign of q), if ever it was present, will be annihilated by the same background. Though, the vacuum is just the void with nothing to be annihilated. The creation rate of the spherical membranes is the same over all the latitudes (Fig. 7(b)). The spherical symmetry of the spatial 3-sphere of de Sitter and the fact that the above result does not depend on the latitudinal position of the membranes imply the random creation of the spherical membranes of random sizes over the spatial 3-sphere (Fig. 7(c)).

4.2 Spherical M2 Branes and the Cosmological Constant Problem

Let us consider the physical implication of the condensation of the spherical membranes. Though it is difficult to compute the back reaction of the condensation in the present setup, one can think of its qualitative consequence. The condensation of the

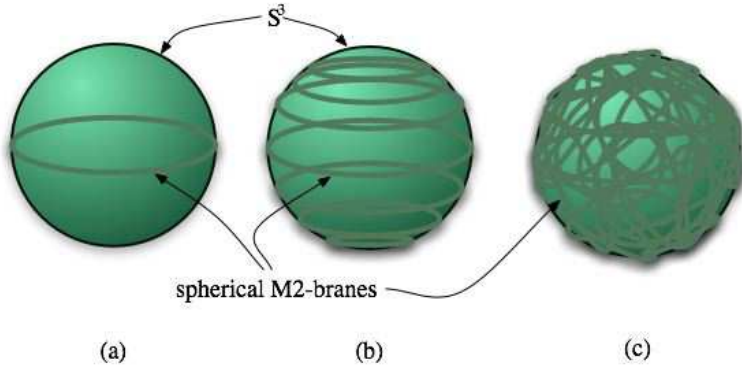


Figure 7: The condensation of spherical membranes over S^3 , the spatial part of de Sitter.

spherical membranes provides us with a natural mechanism to explain the cosmological constant problem, that is, why the cosmological constant is almost vanishing but not completely. The tension of the created spherical membranes will squeeze the accelerating spatial 3-sphere of de Sitter space-time à la Brandenberger-Vafa mechanism [50], which results in the reduction of the cosmological constant. (See also [51] and [52] for detailed analysis.) This is similar to the reheating procedure where matters nucleate as the inflation stops. Here, the condensation of the spherical membranes extracts energy from de Sitter background, which lowers the cosmological constant⁵. The created spherical membranes in this manner could provide the seed of matters.

This procedure cannot exhaust the cosmological constant completely. Recall that the Schwinger pair creation process does not violate the charge conservation. Despite of the condensation of the spherical membranes (with vanishing net M2 charge), the electric flux density ‘ i ’ over the spatial 7-hyperboloid should be invariant. This implies that the resultant geometry of the condensation of the spherical membranes cannot be completely flat Minkowski space-time where the imaginary electric flux is absent. Though the cosmological constant approaches to ‘0’ from above, it cannot vanish completely. This could be one explanation of the cosmological constant problem.

5. Bubble Nucleation

5.1 Bubbles vs. Instability of Kaluza-Klein Vacua

In this subsection, we look into the origin of the bubble nucleation. Let us first see the possibility of the bubble nucleation due to any semi-classical instability of Kaluza-Klein vacuum as we observe in the Witten bubble case [29]. More specifically, we restrict our focus on the Kaluza-Klein compactification involved in M5-bubble solutions. The analyses for other cases will be straightforward.

⁵Some of the early ideas of neutralizing the cosmological constant were considered in Refs. [53] [54] [55] [56].

Kaluza-Klein compactification $M^{9+1} \times S^1$ is classically stable (against small oscillations). In order to check its semi-classical stability, that is, to check any possible penetration to other vacua, we resort to the analysis in Euclidean space. This method is summarized as two steps. First, look for a bounce solution (a Euclidean solution asymptotically approaching $M^{10} \times S^1$). One way to find the Euclidean solution is to take Wick rotation on a known solution in M^{10+1} and make the formerly temporal coordinate compact with appropriate periodicity to achieve the geodesic completeness. Second, check the possibility of the negative modes for small oscillations around the solution. Instead of this latter step, one can directly find the solution into which the ‘false vacuum’ decay [29]. The solution turns out to be Lorentzian solution found by the analytic continuation from Euclidean bounce solution found in the first step. The upshot is that the solution into which the geometry $M^{9+1} \times S^1$ tunnels into semi-classically can be found by taking DWR on a known solution in M^{10+1} dimensions. In all, $M^{9+1} \times S^1$ is a classically stable vacuum but could be semi-classically unstable and possibly decays into M2- or M5-bubble geometry.

One very important thing in this argument is whether these new geometries have the same energy, that is vanishing, as that of the ‘would-be’ unstable $M^{9+1} \times S^1$ vacuum. They do not seem so. We first note that the relation between M-theory in eleven dimensions and the string theory in ten dimensions is not like ordinary Kaluza-Klein style. In order to make sense of ten dimensional theory by the compactification, we have to use a very specific compactification scheme. Regarding the direction ξ as the eleventh dimension circle, the resulting geometry is D4-bubble in IIA;

$$ds^2 = e^{\frac{\phi}{2}} ds_E^2 = H^{-\frac{1}{2}}(r) \sum_{i=1}^5 (dx^i)^2 + H^{\frac{1}{2}}(r) (-r^2 d\psi^2 + dr^2 + r^2 \cosh^2 \psi d\Omega_3^2)$$

$$e^{\phi(r)} = H^{-\frac{1}{4}}(r), \quad F^{(4)} = -3iQ \cosh^3 \psi d\psi \wedge d\Omega_3, \quad H(r) = 1 + \frac{Q}{r^3}. \quad (5.1)$$

The energy-momentum tensor (computed in ten dimensional Einstein frame metric ds_E^2) is

$$T_{\mu\nu} = \frac{1}{2} \left(\partial_\mu \phi \partial_\nu \phi - \frac{g_{E\mu\nu}}{2} \partial_\lambda \phi \partial^\lambda \phi \right)$$

$$+ \frac{e^{\frac{\phi}{2}}}{2 \cdot 4!} \left(4F_{\mu\rho_1\rho_2\rho_3} F_\nu^{\rho_1\rho_2\rho_3} - \frac{g_{E\mu\nu}}{2} F_{\rho_1\rho_2\rho_3\rho_4} F^{\rho_1\rho_2\rho_3\rho_4} \right). \quad (5.2)$$

Computing the component $T_{\psi\psi}$, we get the following result;

$$T_{\psi\psi} = \frac{r^2 H^{-2}}{4 \cdot 16} (\partial_r H)^2 + \frac{H^{-\frac{1}{8}}}{4} \left(H^{\frac{5}{8}} r^2 \cosh^2 \psi \right)^{-3} \left(F_{\psi\Omega} \right)^2$$

$$= \frac{9Q^2 r^{-6} H^{-2}}{4 \cdot 16} - \frac{9Q^2 r^{-6} H^{-2}}{4} = -\frac{3^3 \cdot 5Q^2 r^{-6} H^{-2}}{2^6}. \quad (5.3)$$

The contribution from the imaginary RR four form field results in the negative energy in lower dimensions.

The energy difference between the Kaluza-Klein vacuum and the bubble solutions implies that the latter is not due to any semi-classical instability of the former. This becomes indeed clear if we see RR-form flux that the bubbles carry. There is no such a conserved (though imaginary valued) RR-form flux involved in the Kaluza-Klein vacuum. Moreover, the negative energy of the solution read off in ten-dimensions is not actually concerned with the compactification. In the next subsection, we check the energy condition of M5-bubble solutions directly in eleven dimensions.

5.2 Energy Condition of the Bubbles

The energy-momentum tensor can be easily read from the supergravity action

$$S = \frac{1}{16\pi G_N^{11}} \int d^{11}x \sqrt{-g} \left(R - \frac{1}{2 \cdot 4!} |\mathcal{F}_{(4)}|^2 - \frac{1}{6 \cdot 4! \cdot 4! \cdot 3!} \epsilon \cdot \mathcal{F}_{(4)} \cdot \mathcal{F}_{(4)} \cdot C_{(3)} \right). \quad (5.4)$$

as

$$T_{\mu\nu} = \frac{1}{2 \cdot 3!} \mathcal{F}_{\mu\rho\sigma\kappa} \mathcal{F}_{\nu}^{\rho\sigma\kappa} - \frac{g_{\mu\nu}}{2 \cdot 2 \cdot 4!} \mathcal{F}_{\lambda\rho\sigma\kappa} \mathcal{F}^{\lambda\rho\sigma\kappa}. \quad (5.5)$$

Since

$$\begin{aligned} \mathcal{F}_{\lambda\rho\sigma\kappa} \mathcal{F}^{\lambda\rho\sigma\kappa} &= 4! g^{\psi\psi} g^{\vec{\Omega}_3 \vec{\Omega}_3} (-3iQ \cosh^3 \psi)^2 \\ &= -4! H^{-\frac{2}{3}} r^{-2} \left(H^{-\frac{2}{3}} r^{-2} \cosh^{-2} \right)^3 (-3iQ \cosh^3 \psi)^2 \\ &= 4! \cdot 9Q^2 \left(H^{-\frac{2}{3}} r^{-2} \right)^4, \end{aligned} \quad (5.6)$$

and

$$\mathcal{F}_{\mu\rho\sigma\kappa} \mathcal{F}_{\nu}^{\rho\sigma\kappa} = \begin{cases} 0 & (\mu, \nu \in \{\xi, \vec{x}, r\}) \\ 3! \cdot 9Q^2 \left(H^{-\frac{2}{3}} r^{-2} \right)^4 g_{\mu\nu} & (\mu, \nu \in \{\psi, \vec{\Omega}\}) \end{cases} \quad (5.7)$$

the components of the energy-momentum tensor will be

$$T_{\mu\nu} = \begin{cases} -\frac{9Q^2}{4} \left(H^{-\frac{2}{3}} r^{-2} \right)^4 g_{\mu\nu} & (\mu, \nu \in \{\xi, \vec{x}, r\}) \\ \frac{9Q^2}{4} \left(H^{-\frac{2}{3}} r^{-2} \right)^4 g_{\mu\nu} & (\mu, \nu \in \{\psi, \vec{\Omega}\}) \end{cases} \quad (5.8)$$

The expression becomes more succinct in the orthonormal frame;

$$T_{ab} = \frac{9Q^2}{4} H^{-\frac{8}{3}} r^{-8} \text{diag} \left(\underbrace{-1}_{\xi}, \underbrace{-1, -1, -1, -1, -1}_{\vec{x}}, \underbrace{-1}_{r}, \underbrace{-1}_{\psi}, \underbrace{1, 1, 1}_{\vec{\Omega}} \right). \quad (5.9)$$

The energy density ρ is negative and the pressure p along Euclidean world volume and the radial direction is negative while the pressure along 3-sphere is positive. The geometry therefore violates both the weak energy condition (because $T_{00} < 0$) and

the strong energy condition (because $T_{00} - \eta_{00}T/2 < 0$). The null energy condition is violated for the null direction concerning the coordinates (ξ, \vec{x}, r) but is safe for the null direction involving the spherical coordinates.

This result is in contrast with the case of D/M-branes. The energy-momentum tensor of M5-branes in the orthonormal frame is

$$T_{ab} = \frac{9Q^2}{4} H^{-\frac{8}{3}} r^{-8} \text{diag} \left(\underbrace{1}_t, \underbrace{-1, -1, -1, -1, -1}_x, \underbrace{-1}_r, \underbrace{1, 1, 1, 1}_{\vec{\Omega}} \right), \quad (5.10)$$

thus satisfies the weak energy condition ($T_{00} > 0$), but violates the strong energy condition (because $T_{00} - \eta_{00}T/2 < 0$). It also satisfies the null energy condition ($T_{++} \geq 0$).

The equation of state parameter $w = p/\rho$ reveals very peculiar feature of the solution. It is either 1 or -1 depending on the directions. In the near-bubble regime, the factor in front of the energy-momentum tensor becomes constant, that is,

$$\frac{9Q^2}{4} H^{-\frac{8}{3}} r^{-8} \simeq \frac{9Q^{-\frac{2}{3}}}{4} \quad (5.11)$$

so that the geometry becomes factorized into 7-hyperboloid and $(3+1)$ -de Sitter;

$$R_{ab} = T_{ab} - \frac{1}{9} \eta_{ab} T = \frac{3}{2} Q^{-\frac{2}{3}} \text{diag} \left(\underbrace{-1}_{\xi}, \underbrace{-1, -1, -1, -1, -1}_x, \underbrace{-1}_r, \underbrace{-2, 2, 2, 2}_{\psi, \vec{\Omega}} \right) \quad (5.12)$$

This implies that the equation of state parameter $w = -1$, read from the directions $(\psi, \vec{\Omega})$ of (5.8) in the near bubble regime, looks to be concerned with the cosmological constant. However, the sign of Einstein tensor ($G_{ab} = 9Q^{-\frac{2}{3}}\eta_{ab}/4$) for dS₃₊₁ part in the full eleven dimensional solution, is opposite to that for pure $(3+1)$ -dimensional de Sitter space-time ($G_{ab} = -3Q^{-\frac{2}{3}}\eta_{ab}$). The same is true for the anti-de Sitter compactification of D-brane geometry. Therefore we are not quite sure of the meaning of the equation of state parameter $w = -1$ in these kinds of compactifications. At the least, it is different from that of phantoms ($w < -1$) and accords with the empirical data on the dominant contribution of the matter component [1][2]. Even though we have imaginary fields, thus can be regarded as fields with the kinetic term with the wrong sign, its trivial dynamics ($\mathcal{F}_{(4)}$ is constant) makes the equation of state parameter w different from that of the ordinary phantom fields, and its status phenomenologically safe in the sense discussed in Ref. [18].

6. Extending Hartle-Hawking to Extra Dimensions

We rather interpret the bubble solution just literally as the solution coming from the geometry, ‘anti-de Sitter \times sphere’ via DWR. In other word, we regard DWR

not just as a mathematical tool (to generate a new solution from a given solution) but as a physical process like quantum tunneling. This is very analogous to Hartle-Hawking proposal on the creation of the Universe, which describes de Sitter space-time tunneling from the sphere [38]. The bubble solution adds the hyperbolic space as another ingredient. It tunnels from anti-de Sitter space-time.

In order to be more precise about the surgery of Riemannian geometry and Lorentzian geometry, let us describe the situation in the language of the complex geometry. From here on, we will closely follow the argument developed in [57] and apply it to the case at hand.

The near-bubble geometry $2M_I \equiv dS_{3+1} \times H^7$ we obtained can be considered as the double manifold (obtained by joining two copies, M_I^+ and M_I^- of a manifold M_I , across their common boundary Σ_I) defined in [57]. The near-horizon geometry $S^4 \times AdS_{6+1}$ of the M5-brane cousin is another double manifold $2M_{II}$ appearing in our story.

Both double manifolds are the fixed point sets of two anti-holomorphic involutions, respectively. Let us consider a complex manifold $\mathcal{M}_5 \times \mathcal{M}_8$ and embed two hypersurfaces by the following two complex quadrics;

$$\sum_{i=1}^5 Z_i^2 = l_4^2, \quad \sum_{j=1}^8 W_j^2 = -l_7^2. \quad (6.1)$$

The manifold $2M_I$ is the fixed point set of the anti-holomorphic involution,

$$\begin{aligned} J_I : \quad & (Z_1, Z_2, \dots, Z_5; W_1, W_2, \dots, W_8) \\ & \rightarrow (\bar{Z}_1, \bar{Z}_2, \dots, -\bar{Z}_5; -\bar{W}_1, \bar{W}_2, \dots, \bar{W}_8), \end{aligned} \quad (6.2)$$

while the manifold $2M_{II}$ is the fixed point set of another anti-holomorphic involution,

$$\begin{aligned} J_{II} : \quad & (Z_1, Z_2, \dots, Z_5; W_1, W_2, \dots, W_8) \\ & \rightarrow (\bar{Z}_1, \bar{Z}_2, \dots, \bar{Z}_5; -\bar{W}_1, \bar{W}_2, \dots, -\bar{W}_8). \end{aligned} \quad (6.3)$$

Both double manifolds compose two real slices embedded into the complex manifold $\mathcal{M}_5 \times \mathcal{M}_8$ ('real' in the sense that the metrics pulled back on them are real valued). The intersection of these fixed point sets is therefore given by

$$\sum_{i=1}^4 Z_i^2 = l_4^2, \quad -W_1^2 + \sum_{j=2}^7 W_j^2 = -l_7^2 \quad (6.4)$$

with all Z_i ($i = 1, 2, \dots, 4$) and W_j ($j = 1, 2, \dots, 7$) real, thus defining $S^3 \times H^6$. The anti-holomorphic involution J_{II} acting on $2M_I$ exchanges M_I^+ with M_I^- , while the involution J_I swaps M_{II}^+ with M_{II}^- when it acts on $2M_{II}$. These correspond to the orientation-flip or time-reverse operations. According to the argument in [57], there

is no distributional contribution to Ricci tensor R_{ab} at the intersection, $S^3 \times H^6$, that is, the fixed point set of both involutions J_I and J_{II} . Therefore, we can make the junction of M_I^+ (a half of $dS_{3+1} \times H^7$) and M_{II}^- (a half of $S^4 \times AdS_{6+1}$) across their common boundary $S^3 \times H^6$.

To be more specific, let us take the example of the tunneling from $S^2 \times AdS_{1+1}$ to $dS_{1+1} \times H^2$. For the surgery, it is convenient to use the global coordinates which parametrize the sphere and anti-de Sitter, that is $2M_{II}$, as

$$\begin{aligned} Z_1 &= \sin \theta \cos \varphi, & Z_2 &= \sin \theta \sin \varphi, & Z_3 &= \cos \theta & (S^2) \\ W_1 &= \cosh \lambda \cos \tau, & W_2 &= \sinh \lambda, & W_3 &= \cosh \lambda \sin \tau & (AdS_{1+1}) \end{aligned} \quad (6.5)$$

so that the embedding coordinates satisfy $Z_1^2 + Z_2^2 + Z_3^2 = 1$ (sphere) and $-W_1^2 + W_2^2 - W_3^2 = -1$ (anti-de Sitter). The coordinates for the hyperboloid and de Sitter, viz., $2M_I$ in the above, will be

$$\begin{aligned} Z_1 &= \cosh \psi \cos \varphi, & Z_2 &= \cosh \psi \sin \varphi, & Z_3 &= \sinh \psi & (dS_{1+1}) \\ W_1 &= \cosh \lambda \cosh \mu, & W_2 &= \sinh \lambda, & W_3 &= \cosh \lambda \sinh \mu & (H^2) \end{aligned} \quad (6.6)$$

These latter sets satisfy $Z_1^2 + Z_2^2 - Z_3^2 = 1$ (de Sitter) and $-W_1^2 + W_2^2 + W_3^2 = -1$ (hyperboloid). The involutions J_I and J_{II} defined in (6.2) and (6.3) leave the doubles $2M_I$ and $2M_{II}$, invariant respectively. However, the involution J_I acting on $2M_{II}$, and J_{II} acting on M_I result in the changes $Z_3 \rightarrow -Z_3$ and $W_3 \rightarrow -W_3$. The fixed points (where $Z_3 = W_3 = 0$) of these mappings are specified by $\tau = -i\mu = 0$ and $\theta = i\psi + \pi/2 = \pi/2$, where one can make the junction of M_{II}^- ($\tau < 0, \theta > \pi/2$) and M_I^+ ($\psi > 0, \mu > 0$).

After the surgery, the geometry looks like Fig. 8. The left figure (a) shows the anti-de Sitter tunneling to the hyperbolic space while the right figure (b) illustrates the familiar Hartle-Hawking tunneling from the sphere to de Sitter.

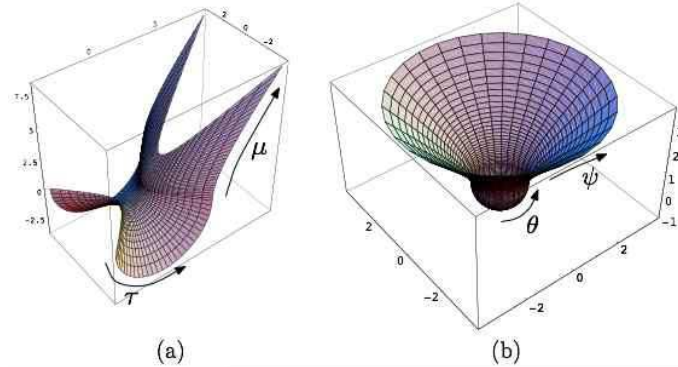


Figure 8: Extension of Hartle-Hawking: (a) anti-de Sitter tunnels to a hyperbolic space, (b) the familiar Hartle-Hawking tunneling process from a sphere to de Sitter

There are some features to note in this example. First, the actual anti-de Sitter space-time is the universal covering space of the corresponding part shown in the

figure. Second, the coordinates (λ, μ) in the hyperbolic part are different from the coordinates (r, ξ) used so far. The part glued to anti-de Sitter space-time in the figure is Poincaré (Lobachevsky) half-plane and therefore the angular coordinate ξ runs from 0 to π , that is to say, Kaluza-Klein internal space is not a circle but an interval (S^1/\mathbf{Z}_2) . In other words, the ‘AdS Universe’ is destined to the hyperboloid compactified on a half circle S^1/\mathbf{Z}_2 . This feature is common to all other bubble solutions discussed in this paper. Especially the standard M-compactification of the M2- or M5-bubble backgrounds will lead to the heterotic bubble vacuum in 10-dimensions. Third, we have to worry about the radial fluctuation (along r) which could invalidate the compactification scheme. Fortunately, this can be controlled by considering the compact (closed) hyperbolic space. General n -dimensional hyperboloid and anti-de Sitter manifold have common isometry subgroup $SO(n-1, 1)$ over their common boundary H^{n-1} . In order to stabilize the radial fluctuation, we replace the previous common boundary H^{n-1} with the compact hyperbolic space H^{n-1}/Γ , where $\Gamma = SO(n-1, 1; \mathbf{Z})$. Then all the radial modes will be confined to Lobachevsky space. See Refs. [58][59] for details about the compact hyperbolic extra dimensions and the radion stabilization.

7. Discussions

In this paper, we showed that most well-known D/M-brane configurations have their bubble cousins. They have a universal feature of having de Sitter space-times as near-bubble geometries. Especially in the extremal cases, these near-bubble de Sitter space-times are exact solutions of 10- or 11-dimensional supergravity theories.

The bubble solutions are obtained by taking DWR on D-branes or M-branes. Especially D-bubbles can also be obtained via timelike T-duality. For example, the extremal D3-bubbles are nothing but Hull’s E4-branes in IIB theory. As for M-bubbles, DWR is a powerful tool to generate bubble solutions because there is no notion of T-duality in M-theory.

It is surprising that the near-bubble geometries of the extremal M5-, M2-, or D3-bubbles preserve 32 supersymmetries (for D1-D5-bubble case, 16 supersymmetries). The imaginary higher-form fields guarantee Killing spinors even in de Sitter backgrounds. Therefore, the bubble solution is the domain wall solution interpolating two maximally supersymmetric regions, i.e., the asymptotic flat Minkowski region and the near-bubble $dS \times H$ region.

Especially supersymmetry makes sense of multi-bubble solutions obtained from multi-brane solutions via DWR. Though the observer can see the bubbles start inflating, once they invade the region near to the observer, each bubble will remain just as a deep throat of de Sitter space-time and it will take infinite coordinate time (affine parameter) for the bubbles to swallow up the whole space-time. At the final stage, the observer will find himself in a grand Swiss-cheese universe, where the effec-

tive cosmological constant varies from point to point near the cheese holes. This is a stringy realization of the multiverse idea that has drawn much interests [60][61][62]. The inflating bubbles leave behind the landscape of de Sitter skeleton.

A fine virtue of this Swiss-cheese uiniverse is that there is a mechanism to control the cosmological constant to almost vanishing values. The imaginary field strengths triggers the creation of spherical D3-, M5-, M2 branes over the spatial section (S^4 , S^6 , S^3) of de Sitter space-time near D3-, M2-, M5-bubbles, respectively. As thus-created spherical branes condense, their tensions decelerate the expansion of de Sitter lowering the cosmological ‘constant’ effectively. Though the effective cosmological constant decreases with the condensation of the spherical branes, the conservation of the fluxes ‘ $\pm i$ ’ of higher-form fields obstructs it to be completely vanishing.

Lastly, we give a few comments on some topics of keen interests.

- **Space-time Dimensionality**

The de Sitter compactification near bubble walls provide us with a natural explanation about why our space-time is of four dimensions. The M5-bubble solution is singled out of other bubble solutions as a model describing our Universe. It actually has some distinctive features from others. Together with the M2-bubble, it is a solution of 11-dimensional supergravity, the low energy limit of M-theory that is currently considered as ‘the theory of everything’. Although both M-bubbles are geodesically complete solutions, the M5-bubble is more peculiar in the sense that it comes from the only non-singular solitonic solution, that is, the M5-brane. By ‘solitonic’ we mean, the M5-brane solution does not require any source term in the action. Meanwhile, the M2-brane solution has a degenerate horizon inside which there is a singularity. See [63] for details. Though this inside region is excluded nicely in the M2-bubble solution, we would rather consider the M5-bubble as the solution describing the birth of our Universe from ‘nothing’ (without any source). In this sense, 4-dimensional space-time is more natural.

- **dS/CFT Duality**

Being different from other trials for de Sitter space-time in string/M-theories, the bubble geometry could provide a new setup for dS/CFT holography. Actually, the near-bubble geometry $dS \times H$ has three boundaries, one at the spatial infinity of the (non-compact) hyperbolic space and the others at two temporal boundaries of de Sitter space-time. In principle, the holographic CFT of the bulk geometry can reside at any boundary of those three. However, since the original configuration before DWR had CFT at the boundary of AdS space-time and the information about the spherical part was captured there via global charges, it is likely that de Sitter part coming from the sphere will be in some way dual to the CFT on the boundary of the hyperbolic space. Such a dS/CFT would be different from what has been considered so far [64].

- The Wave Function of the Universe

According to the no-boundary proposal [38], the ground state amplitude of a 3-geometry is Euclidean path integral over all compact positive definite 4-geometries with the 3-geometry as a boundary. Its extension to the general $(n+1)$ -dimensional universe with a specific n -geometry h_{ij} at a spatial section of the universe will be Euclidean path integral over all compact positive definite $(n+1)$ -geometries $g_{\mu\nu}$ with h_{ij} as a boundary;

$$\Psi_0[h] \sim \int_g e^{-I_E(g)}. \quad (7.1)$$

In the case at hand (M5-bubble), the boundary geometry (the spatial 10-geometry compactified on a half circle (S^1/\mathbf{Z}_2)) is factorized as $S^3 \times H^6$ so that $I_E(g) = I_{S^4}(g_S) + I_{H^7}(g_H)$ and $\Psi_0[h] = \Psi_S[h_S] \cdot \Psi_H^*[h_H]$. Here complex conjugate, which affects only the overall normalization constant, was taken for the hyperboloid part to account for the time reversal (the death of the ‘AdS Universe’). One can naively use the Euclidean solution characterizing $S^4 \times H^7$ to compute the action $I_E(g)$. However, this scheme will fail because the result will be divergent. In fact, the whole Euclidean action with the solution plugged in is

$$\begin{aligned} I_E &= -\frac{1}{16\pi G_N} \int d^{11}x_E \sqrt{g_E} \left(-R + \frac{1}{2 \cdot 4!} |\mathcal{F}_{(4)}|^2 \right) \\ &= \frac{2}{4! \cdot 3! \cdot 16\pi G_N} \int d^{11}x_E \sqrt{g_E} |\mathcal{F}_{(4)}|^2 \\ &= \frac{2 \cdot 9 \cdot 2\pi^2}{3! \cdot 16\pi G_N} \int d\xi d\vec{x} dr r^2 \sim \infty. \end{aligned} \quad (7.2)$$

The main problem of the no-boundary proposal about the wave function of anti-de Sitter Universe is that its Euclidean partner (the hyperboloid) is not closed manifold. (As we discussed earlier, the same reason destabilizes the radion in the hyperbolic extra-dimensions.) In order to cure this problem, we have to make the hyperboloid compact, as before. At least in (2+1)-dimensions, thus compactified hyperboloid becomes Riemann surface with genus $g \geq 2$ and gives a finite answer [65][66]. We will elaborate on this in the forthcoming paper [67].

Acknowledgments

We thank Seungjoon Hyun, Wontae Kim, Sunggeun Lee, and Boris Pioline for valuable comments and discussions. This work is supported in part by Korea Research Foundation through Project No. KRF-2003-070-C00011. It is also supported by the Science Research Center Program of the Korea Science and Engineering Foundation through the Center for Quantum space-time(CQÜeST) of Sogang University with grant number R11-2005-021.

A. Action under the Double Wick Rotation (DWR)

Let us investigate the generic behavior of the supergravity action under a certain multiple Wick rotation. We first note that any multiple Wick rotation can be described in the following compact form;

$$\tilde{e}^a = \lambda^{(a)} e^a, \quad \tilde{\eta}_{ab} = (\lambda^{(a)})^{-2} \eta_{ab}. \quad (\text{A.1})$$

Here the index a is not dummy and $\lambda^{(a)} = \pm i$ depending on the scheme of Wick rotation. The result we derive below is valid even for the general scaling that needs not to be isotropic. The structure coefficient C^a_{bc} defined by

$$de^a = \frac{1}{2} C^a_{bc} e^b \wedge e^c \quad (\text{A.2})$$

transforms as

$$\tilde{C}_{abc} = \frac{1}{\lambda^{(a)} \lambda^{(b)} \lambda^{(c)}} C_{abc}, \quad (\text{A.3})$$

which leads to the transformation of the spin connection components;

$$\tilde{\omega}_{abc} = \frac{1}{2} \left(\tilde{C}_{abc} - \tilde{C}_{bac} - \tilde{C}_{cab} \right) = \frac{1}{\lambda^{(a)} \lambda^{(b)} \lambda^{(c)}} \omega_{abc}. \quad (\text{A.4})$$

From the spin connection one form

$$\tilde{\omega}_{ab}^{(1)} = \tilde{\omega}_{abc} \tilde{e}^c, \quad (\text{A.5})$$

we note that

$$\tilde{\omega}^{(1)a}{}_b = \tilde{\eta}^{ac} \tilde{\omega}_{cb}^{(1)} = (\lambda^{(a)})^2 \eta^{ac} \frac{1}{\lambda^{(c)} \lambda^{(b)}} \omega_{cb}^{(1)} = \frac{\lambda^{(a)}}{\lambda^{(b)}} \omega^{(1)a}{}_b, \quad (\text{A.6})$$

and Riemann tensor two form becomes

$$\tilde{R}_{ab}^{(2)} = d\tilde{\omega}_{ab}^{(1)} + \tilde{\omega}_{ac}^{(1)} \wedge \tilde{\omega}_{cb}^{(1)} = \frac{1}{\lambda^{(a)} \lambda^{(b)}} R_{ab}^{(2)}, \quad (\text{A.7})$$

whose components transform as

$$\tilde{R}_{abcd} = \frac{1}{\lambda^{(a)} \lambda^{(b)} \lambda^{(c)} \lambda^{(d)}} R_{abcd}. \quad (\text{A.8})$$

Ricci tensor transforms as

$$\tilde{R}_{ac} = \frac{1}{\lambda^{(a)} \lambda^{(c)}} R_{ac}. \quad (\text{A.9})$$

Hence the curvature scalar is invariant under any Wick rotation;

$$\tilde{R} = \tilde{\eta}^{ac} \tilde{R}_{ac} = (\lambda^{(a)})^2 \frac{1}{\lambda^{(a)} \lambda^{(c)}} \eta^{ac} R_{ac} = R. \quad (\text{A.10})$$

We see this invariance of the curvature scalar under Wick rotations in the example of anti-de Sitter space-time and the hyperbolic space, also in the case of de Sitter space-time and the sphere.

Maxwell term is also invariant under any Wick rotation. Since

$$\begin{aligned}\tilde{F}^{(2)} &= \frac{1}{2}\tilde{F}_{ab}\tilde{e}^a \wedge \tilde{e}^b = \frac{1}{2}\tilde{F}_{ab}\lambda^{(a)}\lambda^{(b)}e^a \wedge e^b \\ \Rightarrow F_{ab} &= \lambda^{(a)}\lambda^{(b)}\tilde{F}_{ab},\end{aligned}\quad (\text{A.11})$$

one can then easily see

$$F_{ab}F^{ab} = \eta^{ac}\eta^{bd}F_{ab}F_{cd} = (\lambda^{(a)}\lambda^{(b)})^{-2}\tilde{\eta}^{ac}\tilde{\eta}^{bd}\lambda^{(a)}\lambda^{(b)}\lambda^{(c)}\lambda^{(d)}\tilde{F}_{ab}\tilde{F}_{cd} = \tilde{F}_{ab}\tilde{F}^{ab}. \quad (\text{A.12})$$

The same procedure can be applied to the higher form field to see that

$$\tilde{F}_{a_1 a_2 \dots a_n}^{(n)} = \frac{1}{\lambda^{(a_1)}\lambda^{(a_2)}\dots\lambda^{(a_n)}} F_{a_1 a_2 \dots a_n}^{(n)}. \quad (\text{A.13})$$

Especially for the double Wick rotation, Jacobian factor in the volume is invariant because

$$\tilde{e}^1 \wedge \tilde{e}^2 \wedge \dots \wedge \tilde{e}^d = \lambda^{(1)}\lambda^{(2)}\dots\lambda^{(d)}e^1 \wedge e^2 \wedge \dots \wedge e^d = e^1 \wedge e^2 \wedge \dots \wedge e^d. \quad (\text{A.14})$$

In the last step of the above equation, we used DWR prescription of $\tilde{e}^0 = -ie^0$ and $\tilde{e}^n = ie^n$ so that $\lambda^{(1)}\lambda^{(2)}\dots\lambda^{(d)} = 1$. Actually, the same result is valid for arbitrary even number of Wick rotations as far as $\lambda^{(1)}\lambda^{(2)}\dots\lambda^{(d)} = 1$. Consequently, the action is invariant under arbitrary scaling or Wick rotation if $\lambda^{(1)}\lambda^{(2)}\dots\lambda^{(d)} = 1$. This symmetry of the action can be used as a method of generating a new solution from a given solution.

B. D/M-bubbles from D/M-brane configurations via DWR

B.1 D1-D5 Bubble

The non-extremal D1-D5 solution in $(5+1)$ -dimensions is

$$\begin{aligned}ds_{E,6}^2 &= H_1^{-\frac{1}{2}}H_5^{-\frac{1}{2}}(-f_{15}dt^2 + dx^2) + H_1^{\frac{1}{2}}H_5^{\frac{1}{2}}(f_{15}^{-1}dr^2 + r^2d\Omega_3^2), \\ A_{(2)} &= (H_1'^{-1} - 1)dt \wedge dx, \quad \mathcal{F}_{(3)} = -\partial_r H_5' d\Omega_3, \quad e^{\phi_6} = 1,\end{aligned}\quad (\text{B.1})$$

where

$$\begin{aligned}H_i &= 1 + \frac{\mu^2 \sinh^2 \alpha_i}{r^2} \quad (i = 1, 5), \quad H_5' = 1 + \frac{\mu^2 \sinh \alpha_5 \cosh \alpha_5}{r^2}, \\ H_1'^{-1} - 1 &= -\frac{\mu^2 \sinh \alpha_1 \cosh \alpha_1}{r^2 + \mu^2 \sinh^2 \alpha_1}, \quad f_{15} = 1 - \frac{\mu^2}{r^2}.\end{aligned}\quad (\text{B.2})$$

The primed function is not to be confused with the derivative of the unprimed one.

We take DWR used in (1.8), to get the following bubble solution,

$$\begin{aligned}ds^2 &= H_1^{-\frac{1}{2}}H_5^{-\frac{1}{2}}(f_{15}d\xi^2 + dx^2) + H_1^{\frac{1}{2}}H_5^{\frac{1}{2}}(f_{15}^{-1}dr^2 - r^2d\psi^2 + r^2 \cosh^2 \psi d\Omega_2^2), \\ A_{(2)} &= -i(H_1'^{-1} - 1)d\xi \wedge dx, \quad \mathcal{F}_{(3)} = -i\partial_r H_5' r^3 \cosh^2 \psi d\psi \wedge d\Omega_2.\end{aligned}\quad (\text{B.3})$$

Taking the limit $u^2 \ll \mu^2$ on the near-bubble coordinate $u^2 \equiv r^2 - \mu^2$, we get the near bubble geometry

$$ds^2 \simeq (\cosh \alpha_1 \cosh \alpha_5) \left(du^2 + \frac{u^2}{\mu^2 \cosh^2 \alpha_1 \cosh^2 \alpha_5} d\xi^2 + \frac{1}{\cosh^2 \alpha_1 \cosh^2 \alpha_5} dx^2 \right) + \mu^2 \cosh \alpha_1 \cosh \alpha_5 (-d\psi^2 + \cosh^2 \psi d\Omega_2^2)$$

$$\mathcal{F}_{(3)} \simeq -\frac{2i \sinh \alpha_1}{\mu^2 \cosh^3 \alpha_1} u du \wedge d\xi \wedge dx + 2i\mu^2 \sinh \alpha_5 \cosh \alpha_5 \cosh^2 \psi d\psi \wedge d\Omega_2. \quad (\text{B.4})$$

The extremal case is attained by limiting $\mu \rightarrow 0$ and $\alpha_i \rightarrow \infty$ so that $\mu^2 \sinh \alpha_i \cosh \alpha_i \simeq \mu^2 \sinh^2 \alpha_i \equiv Q_i$ be finite. Near the bubble boundary ($r \rightarrow 0$), the configuration becomes

$$ds^2 = \frac{r^2}{\sqrt{Q_1 Q_5}} (d\xi^2 + dx^2) + \frac{\sqrt{Q_1 Q_5}}{r^2} (dr^2 - r^2 d\psi^2 + r^2 \cosh^2 \psi d\Omega_2^2)$$

$$\mathcal{F}_{(3)} = -\frac{2i r}{Q_1} dr \wedge d\xi \wedge dx + 2i Q_5 \cosh^2 \psi d\psi \wedge d\Omega_2. \quad (\text{B.5})$$

The electric and magnetic flux over the (ξ, x, r) -direction are respectively

$$\int * \mathcal{F}_{(3)} = \int \frac{2i Q_5 r}{(r^2 + Q_1)(r^2 + Q_5)} dr \wedge d\xi \wedge dx = \frac{i \ln \frac{Q_1}{Q_5}}{\frac{Q_1}{Q_5} - 1} \int d\xi \wedge dx,$$

$$\int \mathcal{F}_{(3)} = - \int \frac{2i Q_1 r}{(r^2 + Q_1)^2} dr \wedge d\xi \wedge dx = -i \int d\xi \wedge dx. \quad (\text{B.6})$$

The dependence of the electric flux on Q_1 , as well as Q_5 , is surprising. This is in contrast with D1-D5 branes on T^4 , where the electric and the magnetic flux are given by

$$\int_{S^3} * H_{(3)} = -2Q_1 \lim_{r \rightarrow \infty} \int \frac{(r^2 + Q_1)(r^2 + Q_5)}{(r^2 + Q_1)^2} d\Omega_3 = -2Q_1 \omega_3,$$

$$\int_{S^3} H_{(3)} = 2Q_5 \lim_{r \rightarrow \infty} \int d\Omega_3 = 2Q_5 \omega_3. \quad (\text{B.7})$$

Here ω_n stands for the volume of a unit n -sphere. Although the electric flux involves both Q_1 and Q_5 , the final result depends only on Q_1 .

B.2 M2-Bubble

Non-extremal M2 solution takes the form;

$$ds^2 = H_T^{-\frac{2}{3}}(r) \left(-dt^2 f_T(r) + \sum_{i=1}^2 dx_i^2 \right) + H_T^{\frac{1}{3}}(r) (dr^2 f_T^{-1}(r) + r^2 d\Omega_7^2), \quad (\text{B.8})$$

and 3-form connection field is given by

$$C_{t12} = H_T'^{-1} - 1 = -\frac{\mu_T^6 \sinh \alpha_T \cosh \alpha_T}{r^6} H_T^{-1}. \quad (\text{B.9})$$

The explicit form of the harmonic functions are

$$f_T(r) = 1 - \frac{\mu_T^6}{r^6}, \quad H_T(r) = 1 + \frac{\mu_T^6 \sinh^2 \alpha_T}{r^6}. \quad (\text{B.10})$$

4-form field strength constructed from the above connection is

$$\mathcal{F}_{(4)} = dC_3 = -\frac{6H_T^{-2}\mu_T^6 \sinh \alpha_T \cosh \alpha_T}{r^7} dt \wedge dx^1 \wedge dx^2 \wedge dr. \quad (\text{B.11})$$

After double Wick rotations (one along the temporal direction and the other along one of the spherical directions) as in (1.8), we obtain the following bubble solution;

$$\begin{aligned} ds^2 &= H_T^{-\frac{2}{3}}(r) (f_T(r)d\xi^2 + dx_1^2 + dx_2^2) + H_T^{\frac{1}{3}}(r) (f_T^{-1}(r)dr^2 - r^2 d\psi^2 + r^2 \cosh^2 \psi d\Omega_6^2), \\ \mathcal{F}_{(4)} &= \frac{6i H_T^{-2}\mu_T^6 \sinh \alpha_T \cosh \alpha_T}{r^7} d\xi \wedge dx^1 \wedge dx^2 \wedge dr. \end{aligned} \quad (\text{B.12})$$

In the near-bubble coordinate ($u^2 = r^6 - \mu_T^6$, $u^2 \ll \mu_T^6$), one can approximate the solution as

$$\begin{aligned} ds^2 &\simeq \frac{\cosh^{\frac{2}{3}} \alpha_T}{9\mu_T^4} \left(du^2 + \frac{9u^2}{\mu_T^2 \cosh^2 \alpha_T} d\xi^2 \right) + \cosh^{-\frac{4}{3}} \alpha_T (dx_1^2 + dx_2^2) \\ &\quad + \mu_T^2 \cosh^{\frac{2}{3}} \alpha_T (-d\psi^2 + \cosh^2 \psi d\Omega_6^2), \\ \mathcal{F}_{(4)} &\simeq \frac{2i \sinh \alpha_T}{\mu_T^6 \cosh^3 \alpha_T} u d\xi \wedge dx^1 \wedge dx^2 \wedge du. \end{aligned} \quad (\text{B.13})$$

In order for the geometry to be geodesically complete, the compact direction ($\xi \sim \xi + 2\pi\hat{R}$) should have a period $\hat{R} = \mu_T \cosh \alpha_T / 3$. For this value of \hat{R} , the geometry is factorized as $D_2 \times \mathbf{R}^2 \times dS_{6+1}$, where the cosmological constant of de Sitter space-time is $\Lambda_{6+1} = 15/\mu_T^2 \cosh^{\frac{2}{3}} \alpha_T$.

Taking the limit $\mu_T \rightarrow 0$ and $\alpha_T \rightarrow \infty$ and keeping $Q_T = \mu_T^6 \sinh \alpha_T \cosh \alpha_T$ finite, we obtain the extremal near-bubble configuration as an exact solution;

$$\begin{aligned} ds^2 &= \frac{Q_T^{\frac{1}{3}}}{9\mu_T^6} \left(du^2 + \frac{9\mu_T^4 u^2}{Q_T} d\xi^2 \right) + \frac{\mu_T^4}{Q_T^{\frac{2}{3}}} (dx_1^2 + dx_2^2) + Q_T^{\frac{1}{3}} (-d\psi^2 + \cosh^2 \psi d\Omega_6^2), \\ \mathcal{F}_{(4)} &= \frac{2i}{Q_T} u d\xi \wedge dx^1 \wedge dx^2 \wedge du. \end{aligned} \quad (\text{B.14})$$

In this case, the cosmological constant is $\Lambda = 15/Q_T^{\frac{1}{3}}$.

The magnetic flux due to the M2-'instanton' that sources the extremal bubble geometry is

$$\int_{\mathbf{H}_4} \mathcal{F}_{(4)} = \int \frac{6i Q_T}{r^7 H_T^2} d\xi \wedge dx^1 \wedge dx^2 \wedge dr = \text{Vol}_3 \int_0^\infty \frac{6i Q_T r^5 dr}{(r^6 + Q_T)^2} = i \text{Vol}_3.$$

B.3 M5-Bubble

Starting with the non-extremal M5 solution

$$ds^2 = H_F(r)^{-\frac{1}{3}} \left(-dt^2 f_F(r) + \sum_{i=1}^5 dx_i^2 \right) + H_F(r)^{\frac{2}{3}} \left(dr^2 f_F^{-1}(r) + r^2 d\Omega_4^2 \right), \quad (\text{B.15})$$

with the 4-form field

$$\mathcal{F}_{(4)} = *dH'_F = -3\mu_F^3 \sinh \alpha_F \cosh \alpha_F d\Omega_4, \quad (\text{B.16})$$

and taking DWR, we get

$$\begin{aligned} ds^2 &= \frac{H_F^{\frac{2}{3}}(r)}{f_F(r)} \left(dr^2 + \frac{f_F^2(r)}{H_F(r)} d\xi^2 \right) + H_F^{-\frac{1}{3}}(r) \sum_{i=1}^5 dx_i^2 + H_F^{\frac{2}{3}}(r) r^2 (-d\psi^2 + \cosh^2 \psi d\Omega_3^2), \\ \mathcal{F}_{(4)} &= -3i\mu_F^3 \sinh \alpha_F \cosh \alpha_F \cosh^3 \psi d\psi \wedge d\Omega_3. \end{aligned} \quad (\text{B.17})$$

In the above, the harmonic functions are

$$f_F(r) = 1 - \frac{\mu_F^3}{r^3}, \quad H_F(r) = 1 + \frac{\mu_F^3 \sinh^2 \alpha_F}{r^3}, \quad H'_F(r) = 1 + \frac{\mu_F^3 \sinh \alpha_F \cosh \alpha_F}{r^3}.$$

Introducing the near-bubble coordinate as $u^2 \equiv r^3 - \mu_F^3$, and considering the region of $u^2 \ll \mu_F^3$, we get the geometry

$$\begin{aligned} ds^2 &\simeq \frac{4 \cosh^{\frac{4}{3}} \alpha_F}{9\mu_F} \left(du^2 + \frac{9u^2}{4\mu_F^2 \cosh^2 \alpha_F} d\xi^2 \right) + \cosh^{-\frac{2}{3}} \alpha_F \sum_{i=1}^5 dx_i^2 \\ &\quad + \mu_F^2 \cosh^{\frac{4}{3}} \alpha_F (\cosh^2 \psi d\Omega_3^2 - d\psi^2). \end{aligned} \quad (\text{B.18})$$

In order to make the geometry geodesically complete, we have to set the period of the angular coordinate as $\xi \sim \xi + 2\pi\hat{R}$, with $\hat{R} = (2\mu_F \cosh \alpha_F)/3$. The near-bubble geometry is therefore $D_2 \times \mathbf{R}^5 \times dS_{3+1}$.

Taking the extremal limit as $\mu_F \rightarrow 0$ and $\alpha_F \rightarrow \infty$ with $Q \equiv \mu_F^3 \sinh \alpha_F \cosh \alpha_F$ kept finite, and using a new radial coordinate, $r = y^2$, we get

$$\begin{aligned} ds^2 &= 4Q^{\frac{2}{3}} \left(\frac{dy^2}{y^2} + \frac{y^2}{4Q} \left(d\xi^2 + \sum_{i=1}^5 dx_i^2 \right) \right) + Q^{\frac{2}{3}} (-d\psi^2 + \cosh^2 \psi d\Omega_3^2), \\ \mathcal{F}_{(4)} &= -3iQ \cosh^3 \psi d\psi \wedge d\Omega_3. \end{aligned} \quad (\text{B.19})$$

The electric flux over the hyperbolic space is

$$\begin{aligned} \int_{\text{H}_7} * \mathcal{F}_{(4)} &= -3iQ \int_{\text{H}_7} \cosh^3 \psi * (d\psi \wedge d\Omega_3) \\ &= - \int \frac{3iQ}{H_F^2 r^4} d\xi (\wedge_{i=1}^5 dx_i) \wedge dr \\ &= -3iQ \text{Vol}_6 \int_0^\infty \frac{r^2}{(r^3 + Q)^2} dr = -i \text{Vol}_6. \end{aligned} \quad (\text{B.20})$$

C. Supersymmetry in the Near-Bubble Geometry: Details

C.1 Global Coordinates for $\text{AdS}_{(n-1)+1}$ and \mathbf{H}^n

Here, we introduce the global coordinates for anti-de Sitter space-time and the hyperbolic space. One important virtue of these coordinates is that they are dimensionless (a feature convenient for solving Killing spinor equations).

Let us first consider AdS_3 case. Since it is a coset manifold $SO(2, 2)/SO(2, 1)$, one can pick up a hypersurface $-U^2 - V^2 + X^2 + Y^2 = -R^2$ embedded in a flat space-time of signature $(2, 2)$. We fix the length to be timelike so that the surface has $SO(2, 1)$ isometry. (The little group of the timelike line element is $SO(2, 1)$.) The global coordinates for this hypersurface are

$$\begin{aligned} U &= R \cosh \lambda \sin \tau, \\ V &= R \cosh \lambda \cos \tau, \\ X &= R \sinh \lambda \cos \vartheta, \\ Y &= R \sinh \lambda \sin \vartheta. \end{aligned} \tag{C.1}$$

The flat metric induced on the hypersurface is

$$ds^2 = R^2 \left(-\cosh^2 \lambda d\tau^2 + d\lambda^2 + \sinh^2 \lambda d\vartheta^2 \right). \tag{C.2}$$

The hyperbolic space \mathbf{H}^3 , being the coset manifold $SO(3, 1)/SO(3)$, is represented by the hypersurface $\bar{U}^2 - V^2 + X^2 + Y^2 = -R^2$ embedded in a $(3+1)$ -dimensional flat space-time. A proper parametrization for this hypersurface is obtained by Wick rotation $\tau = -i\mu$ from that of AdS_3 space-time;

$$\begin{aligned} U &= -i R \cosh \lambda \sinh \mu \equiv -i\bar{U}, \\ V &= R \cosh \lambda \cosh \mu, \\ X &= R \sinh \lambda \cos \vartheta, \\ Y &= R \sinh \lambda \sin \vartheta. \end{aligned} \tag{C.3}$$

(Another Wick rotation $\tau = -i\mu + \pi/2$ is also possible, which amounts to exchange the role of U and V .) From the metric $ds^2 = d\bar{U}^2 - dV^2 + dX^2 + dY^2$ of the ambient space-time, one can derive the metric induced on the hypersurface;

$$ds^2 = R^2 \left(\cosh^2 \lambda d\mu^2 + d\lambda^2 + \sinh^2 \lambda d\vartheta^2 \right). \tag{C.4}$$

The above global coordinates (C.2) can be easily generalized to higher dimensional cases. The metric of $\text{AdS}_{(n-1)+1}$ space-time in the global coordinates is

$$ds^2 = R^2 \left(-\cosh^2 \lambda d\tau^2 + d\lambda^2 + \sinh^2 \lambda d\Omega_{n-2}^2 \right). \tag{C.5}$$

Wick rotation $\tau = -i\mu$ (or $\tau = -i\mu + \pi/2$) gives the metric of \mathbf{H}^n .

C.2 Spin Connections for the Unit Sphere and the Unit de Sitter

In this subsection, we summarize the method to get spin connections for the symmetric spaces used in the paper. For more complete argument, see Ref. [68]. The n -sphere S^n and the n -dimensional de Sitter space-time $dS_{(n-1)+1}$ are symmetric spaces diffeomorphic to the coset manifold $SO(n+1)/SO(n)$ and $SO(n,1)/SO(n-1,1)$ respectively. Therefore every geometric information can be basically read off from the Lie algebras of those cosets;

$$\begin{aligned} [P_a, M_{bc}] &= \eta_{ab}P_c - \eta_{ac}P_b, \quad (a, b, c, d = 1, 2, \dots, n) \\ [P_a, P_b] &= -M_{ab}, \quad [M_{ab}, M_{cd}] = \eta_{bc}M_{ad} + \eta_{ad}M_{bc} - \eta_{ac}M_{bd} - \eta_{bd}M_{ac}. \end{aligned} \quad (\text{C.6})$$

Here $(\eta_{ab}) = \text{diag}(1, 1, \dots, 1, \zeta)$ with $\zeta = 1$ for the sphere and $\zeta = -1$ for de Sitter.

In these cases, Maurer-Cartan 1-form constructed from the coset representative,

$$u(x^1, \dots, x^n) = e^{x^1 P_1} \cdots e^{x^n P_n}, \quad (\text{C.7})$$

is expanded as the sum of the vielbein 1-form and the spin connection 1-form. From now on in this section, whenever the products of the form $\prod_{a=p}^q f_a$, ($q < p$) appears in any expression, we mean its value is equal to ‘1’, just for the notational convenience. The explicit expression for Maurer-Cartan 1-form is

$$\begin{aligned} u^{-1}du &= dx^n P_n + \sum_{a=1}^{n-1} dx^a P_a \left(\prod_{b=a+1}^{n-1} \cos x^b \right) \cos(\sqrt{\zeta} x^n) \\ &\quad - \sum_{a=1}^{n-1} dx^a \left[M_{a\,n} \left(\prod_{b=a+1}^{n-1} \cos x^b \right) \frac{1}{\sqrt{\zeta}} \sin(\sqrt{\zeta} x^n) + \sum_{c=a+1}^{n-1} M_{a\,c} \left(\prod_{b=a+1}^{c-1} \cos x^b \right) \sin x^c \right] \\ &= \sum_{a=1}^n P_a e^a + \sum_{a < c} M_{a\,c} \omega^{ac}. \end{aligned} \quad (\text{C.8})$$

The left invariant Riemannian metric on the coset space, being proportional to Killing metric, can be set to $B_{ab} = \eta_{ab}$. The geometry of the coset space, is then described by the following metric

$$\begin{aligned} ds^2 &= B_{ab} e^a e^b = \zeta (dx^n)^2 + \left(dx^{n-1} \cos \sqrt{\zeta} x^n \right)^2 + \sum_{a=1}^{n-2} \left(dx^a \cos \sqrt{\zeta} x^n \prod_{b=a+1}^{n-1} \cos x^b \right)^2 \\ &= \zeta (e^n)^2 + (e^{n-1})^2 + \sum_{a=1}^{n-2} (e^a)^2. \end{aligned} \quad (\text{C.9})$$

For the n -sphere ($\zeta = 1$) or the n -dimensional de Sitter space-time ($\zeta = -1$), the above form of the metric can be related to the standard form by transforming the coordinates;

$$x^1 = \varphi, \quad x^a = \theta_{a-1} - \frac{\pi}{2} \quad (a = 2, \dots, n-1), \quad x^n = \begin{cases} \theta_{n-1} - \pi/2 & (\zeta = 1) \\ \psi & (\zeta = -1) \end{cases} \quad (\text{C.10})$$

C.3 Spin Connections in $\text{AdS}_{(n-1)+1}$ and \mathbf{H}^n

The spin connections are rather easy to compute in the global coordinates if we make use of the results (C.8) and (C.10) for the unit $(n-2)$ -sphere. To be more specific, let us write down the vielbeins first;

$$\begin{aligned} e^0 &= R \cosh \lambda dt, \\ e^1 &= R d\lambda, \\ e^a &= R \sinh \lambda \tilde{e}^{a-1} \quad (2 \leq a \leq n-1), \end{aligned} \quad (\text{C.11})$$

where \tilde{e}^{a-1} denote the vielbeins of the unit sphere used in (C.9) with the convention (C.10). We note that the only difference between anti-de Sitter case and the hyperbolic case is the different signature of $\eta_{00} = \eta$ and the vielbeins take the same form in the above global coordinates with the change of $t \leftrightarrow \xi$ understood. Hereafter, we represent all the results collectively to be applicable for both cases. The frame structure equations $de^a = (C^a_{bc} e^b \wedge e^c)/2$ are

$$\begin{aligned} de^0 &= \frac{\tanh \lambda}{R} e^1 \wedge e^0, \quad de^1 = 0, \\ de^a &= \frac{\coth \lambda}{R} e^1 \wedge e^a + \frac{1}{2R \sinh \lambda} \sum_{b,c \geq 2}^{n-1} \tilde{C}^{a-1}{}_{b-1 c-1} e^b \wedge e^c, \end{aligned} \quad (\text{C.12})$$

where $\tilde{C}^{a-1}{}_{b-1 c-1}$ denotes the frame structure constant of the unit $(n-2)$ -sphere in the standard coordinates (C.9) and the index a runs from 2 to $n-1$. Nontrivial frame structure constants are

$$C^0{}_{10} = \frac{\tanh \lambda}{R}, \quad C^a{}_{1a} = \frac{\coth \lambda}{R}, \quad C^a{}_{bc} = \frac{1}{R \sinh \lambda} \tilde{C}^{a-1}{}_{b-1 c-1}. \quad (\text{C.13})$$

Using (C.11), we get the following non-vanishing spin connection components;

$$\begin{aligned} \omega_{01} &= \frac{\eta}{R} \tanh \lambda e^0 = \eta \sinh \lambda dt \\ \omega_{1a} &= -\frac{\coth \lambda}{R} e^a = -\cosh \lambda d\theta_{a-2} \prod_{b=a-1}^{n-3} \sin \theta_b, \quad (a = 2, \dots, n-2) \\ \omega_{1n-1} &= -\frac{\coth \lambda}{R} e^{n-1} = -\cosh \lambda d\theta_{n-3} \\ \omega_{ab} &= \frac{1}{R \sinh \lambda} \tilde{\omega}_{a-1 b-1 c-1} e^c = \tilde{\omega}_{a-1 b-1}, \quad (a, b = 2, \dots, n-1). \end{aligned} \quad (\text{C.14})$$

We denote $\varphi = \theta_0$ for notational convenience.

The spin connections $\tilde{\omega}_{ab}$ ($a < b$) of the unit $(n-2)$ -sphere are

$$\tilde{\omega}_{ab} = d\theta_{a-1} \left(\prod_{c=a}^{b-2} \sin \theta_c \right) \cos \theta_{b-1} \quad (a = 1, \dots, n-3), \quad (b = a+1, \dots, n-2).$$

Nontrivial components of the curvature tensor are

$$\begin{aligned}
R_{01} &= -\frac{\eta}{R^2} e^0 \wedge e^1, \\
R_{0a} &= -\frac{\eta}{R^2} e^0 \wedge e^a, \\
R_{1a} &= -\frac{1}{R^2} e^1 \wedge e^a + \frac{\cosh \lambda}{R} \left(\omega_{abc} - \frac{1}{2} C_{abc} \right) e^b \wedge e^c = -\frac{1}{R^2} e^1 \wedge e^a, \\
R_{ab} &= \frac{1}{R^2 \sinh^2 \lambda} \left(\tilde{R}_{a-1 b-1 c-1 d-1} - \cosh^2 \lambda (\delta_{ac} \delta_{bd} - \delta_{ad} \delta_{bc}) \right), \tag{C.15}
\end{aligned}$$

where $2 \leq a, b, c, d \leq n-1$. Since both AdS_n and H^n are coset spaces, Ricci tensor is proportional to the metric;

$$R_{00} = -(n-1) \frac{\eta}{R^2}, \quad R_{11} = -(n-1) \frac{1}{R^2}, \quad R_{ab} = -(n-1) \frac{\delta_{ab}}{R^2}. \tag{C.16}$$

C.4 Spin Connections of M5-bubble Background

Let us be specific to the extremal M5-bubble case and obtain the explicit form of the spin connection components. In order to compare the result with that of the extremal M5-branes (whose near-horizon geometry is $\text{AdS}_{6+1} \times \text{S}^4$), we give the expressions of both cases together at every step.

Spin Connections for AdS_{6+1} and H^7

From the foregoing results (C.11), we can easily spell out the explicit forms of the vielbeins for AdS_{6+1} and H_7 involved with the extremal M5 branes/bubbles;

$$\begin{aligned}
e^0 &= 2Q^{\frac{1}{3}} dt \cosh \lambda, \\
e^1 &= 2Q^{\frac{1}{3}} d\lambda, \\
e^a &= 2Q^{\frac{1}{3}} d\theta_{a-2} \sinh \lambda \left(\prod_{b=a-1}^4 \sin \theta_b \right), \quad (a = 2, \dots, 6). \tag{C.17}
\end{aligned}$$

The nontrivial spin connections are

$$\begin{aligned}
\omega_{01} &= \eta dt \sinh \lambda, \\
\omega_{1a} &= -d\theta_{a-2} \cosh \lambda \prod_{b=a-1}^4 \sin \theta_b, \quad (a = 2, \dots, 6) \tag{C.18} \\
\omega_{ab} &= d\theta_{a-2} \cos \theta_{b-2} \prod_{c=b-3}^{a-1} \sin \theta_c, \quad (a = 2, \dots, 5; b = 3, \dots, 6; a+1 \leq b),
\end{aligned}$$

It should be understood that $\eta = \eta_{00} = -1$ for AdS_{6+1} while it is 1 for H_7 .

Spin Connections for S^4 and dS_4

We again use the results (C.8) and (C.10) but with different angular coordinates $(\phi \equiv \chi_0, \chi_1, \chi_2, \chi_3)$ in order to avoid any confusion with the ones used for AdS_{6+1} and S^4 . We use the conventional angular coordinates for S^4 ;

$$e^{a+7} = Q^{\frac{1}{3}} d\chi_a \prod_{b=a+1}^3 \sin \chi_b, \quad (a = 0, \dots, 3). \quad (C.19)$$

According to the Eq. (C.8), the spin connection components read as

$$\omega^{a+7}{}_{b+7} = d\chi_a \cos \chi_b \prod_{c=a+1}^{b-1} \sin \chi_c, \quad (a = 0, 1, 2; \ b = 1, 2, 3; \ a < b). \quad (C.20)$$

For de Sitter case in (C.8), we use $\zeta = -1$. The same results can be obtained via Wick rotation from those of the sphere case. The vielbein e^\sharp goes to $i\bar{e}^\sharp$ upon Wick rotation, $\chi_3 = i\psi + \pi/2$ (where we used \sharp to denote the tenth component). This is because $\bar{\eta}_{\sharp\sharp} = \bar{\eta}^{\sharp\sharp} = \zeta = -1$ while Euclidean flat metric has been used for the sphere. The spin connection $\omega_{ab} = \omega_{abc} e^c$, being constructed from the frame structure constants via $\omega_{abc} = (C_{abc} - C_{bac} - C_{cab})/2$, takes extra i on every occurrence of the subindex ‘ \sharp ’ upon Wick rotation. In all, the above equations are rephrased in de Sitter case as

$$\bar{e}^{a+7} = Q^{\frac{1}{3}} d\chi_a \cosh \psi \prod_{c=a+1}^2 \sin \chi_c, \quad \bar{e}^\sharp = Q^{\frac{1}{3}} d\psi. \quad (C.21)$$

and the spin connection components become

$$\begin{aligned} \bar{\omega}^{a+7}{}_{b+7} &= d\chi_a \cos \chi_b \prod_{c=a+1}^{b-1} \sin \chi_c, \\ \bar{\omega}^{a+7}{}_\sharp &= d\chi_a \sinh \psi \prod_{c=a+1}^2 \sin \chi_c, \quad (a = 0, 1, 2; \ b = 1, 2; \ a < b). \end{aligned} \quad (C.22)$$

The curvature tensor two forms are simply given by $R^{ab} = e^a \wedge e^b / Q^{\frac{2}{3}}$ (and $\bar{R}^{ab} = \bar{e}^a \wedge \bar{e}^b / Q^{\frac{2}{3}}$ for de Sitter), thus with Ricci tensor components as $R_{ab} = 3\delta_{ab}/Q^{\frac{2}{3}}$ for a sphere and $\bar{R}_{ab} = 3\bar{\eta}_{ab}/Q^{\frac{2}{3}}$ for de Sitter.

The explicit forms of the matrices Ω_μ

The explicit forms of the matrices Ω_μ defined in Eq. (3.6) are

$$\begin{aligned}
\Omega_t &= -\eta (\kappa \Gamma^{0789} \cosh \lambda - \Gamma^{01} \sinh \lambda), \\
\Omega_\lambda &= -\kappa \Gamma^{1789}, \\
\Omega_{\theta_a} &= -(\kappa \Gamma^{(a+2)789} \sinh \lambda + \Gamma^{1(a+2)} \cosh \lambda) \left(\prod_{b=a+1}^4 \sin \theta_b \right) + \Gamma^{(a+2)(a+3)} \cos \theta_{a+1} \\
&\quad + \sum_{b=a+2}^4 \Gamma^{(a+2)(b+2)} \cos \theta_b \prod_{c=a+1}^{b-1} \sin \theta_c, \quad (a = 0, \dots, 3) \\
\Omega_{\theta_4} &= -(\kappa \Gamma^{6789} \sinh \lambda + \Gamma^{16} \cosh \lambda), \tag{C.23}
\end{aligned}$$

for $\text{AdS}_{6+1}/\text{H}^7$ parts.

For the sphere, the matrices are

$$\begin{aligned}
\Omega_\phi &= \Gamma^{78} \cos \chi_1 + \Gamma^{79} \sin \chi_1 \cos \chi_2 + \Gamma^{7} \sin \chi_1 \sin \chi_2 \cos \chi_3 + \Gamma^{89} \sin \chi_1 \sin \chi_2 \sin \chi_3, \\
\Omega_{\chi_1} &= \Gamma^{89} \cos \chi_2 + \Gamma^{8} \sin \chi_2 \cos \chi_3 - \Gamma^{79} \sin \chi_2 \sin \chi_3, \\
\Omega_{\chi_2} &= \Gamma^{9} \cos \chi_3 + \Gamma^{78} \sin \chi_3, \\
\Omega_{\chi_3} &= -\Gamma^{789}, \tag{C.24}
\end{aligned}$$

while for de Sitter part, they are

$$\begin{aligned}
\Omega_\phi &= \Gamma^{78} \cos \chi_1 + \Gamma^{79} \sin \chi_1 \cos \chi_2 + \Gamma^{7} \sin \chi_1 \sin \chi_2 \sinh \psi + i \Gamma^{89} \sin \chi_1 \sin \chi_2 \cosh \psi, \\
\Omega_{\chi_1} &= \Gamma^{89} \cos \chi_2 + \Gamma^{8} \sin \chi_2 \sinh \psi - i \Gamma^{79} \sin \chi_2 \cosh \psi, \\
\Omega_{\chi_2} &= \Gamma^{9} \sinh \psi + i \Gamma^{78} \cosh \psi, \\
\Omega_\psi &= -i \Gamma^{789}. \tag{C.25}
\end{aligned}$$

References

- [1] S. Perlmutter et al, *Astrophys. J.*, **517**, 565 (1999) [arXiv:astro-ph/9812133].
- [2] A. G. Riess et al. *Astron. J.*, **116**, 1009 (1998) [arXiv:astro-ph/9805201].
- [3] S. M. Carroll, *Living Rev. Rel.*, **4**, 1 (2001) [arXiv:astro-ph/0004075].
- [4] T. Padmanabhan, *Phys. Rept.*, **380**, 235 (2003) [arXiv:hep-th/0212290].
- [5] S. Weinberg, *Rev. Mod. Phys.* **61**, 1 (1989).
- [6] J. Polchinski, “The cosmological constant and the string landscape,” hep-th/0603249 (2006).
- [7] See for example, V. Balasubramanian, *Class. Quant. Grav.*, **21**, S1337 (2004) [arXiv:hep-th/0404075].

- [8] T. Banks, “Cosmological breaking of supersymmetry? or Little lambda goes back to the future 2,” hep-th/0007146 (2000).
- [9] W. Fischler, A. Kashani-Poor, R. McNees, and S. Paban, *JHEP*, **07**, 003 (2001) [arXiv:hep-th/0104181].
- [10] E. Witten, “Quantum gravity in de sitter space,” hep-th/0106109 (2001).
- [11] R. Bousso, “Adventures in de Sitter space,” hep-th/0205177 (2002).
- [12] N. Goheer, M. Kleban, and L. Susskind, *JHEP*, **07**, 056 (2003) [arXiv:hep-th/0212209].
- [13] J. M. Maldacena and C. Nunez, *Int. J. Mod. Phys.*, **A16**, 822 (2001) [arXiv:hep-th/0007018].
- [14] C. M. Hull, *JHEP*, **07**, 021 (1998) [arXiv:hep-th/9806146].
- [15] F. Hoyle and J. V. Narlikar, *Proc. Royal Soc. London*, **A273**, 1 (1962).
- [16] G. W. Gibbons, “Phantom matter and the cosmological constant,” hep-th/0302199, (2003).
- [17] R. R. Caldwell, *Phys. Lett.*, **B545**, 23 (2002) [arXiv:astro-ph/9908168].
- [18] S. M. Carroll, M. Hoffman and M. Trodden, *Phys. Rev.*, **D68**, 023509 (2003) [arXiv:astro-ph/0301273].
- [19] J. S. Schwinger, *Phys. Rev.*, **82**, 664 (1951).
- [20] E. Mottola, *Phys. Rev.*, **D31**, 754 (1985).
- [21] L. H. Ford, *Phys. Rev.*, **D31**, 710 (1985).
- [22] E. Mottola, *Phys. Rev.*, **D33**, 1616 (1986).
- [23] I. Antoniadis, J. Iliopoulos and T. N. Tomaras, *Phys. Rev. Lett.*, **56**, 1319 (1986).
- [24] J. D. Barrow, *Phys. Lett.*, **B180**, 335 (1986).
- [25] S. B. Giddings, S. Kachru, and J. Polchinski, *Phys. Rev.*, **D66**, 106006 (2002) [arXiv:hep-th/0105097].
- [26] P. K. Townsend and M. N. R. Wohlfarth, *Phys. Rev. Lett.*, **91**, 061302 (2003) [arXiv:hep-th/0303097].
- [27] S. Kachru, R. Kallosh, A. Linde, and S. P. Trivedi, *Phys. Rev.*, **D68**, 046005 (2003) [arXiv:hep-th/0301240].
- [28] L. Susskind, “The anthropic landscape of string theory,” hep-th/0302219, (2003).
- [29] E. Witten, *Nucl. Phys.*, **B195**, 481 (1982).

- [30] O. Aharony, M. Fabinger, G. T. Horowitz and E. Silverstein, *JHEP* **0207**, 007 (2002) [arXiv:hep-th/0204158].
- [31] V. Balasubramanian, K. Larjo and J. Simon, *Class. Quant. Grav.* **22**, 4149 (2005) [arXiv:hep-th/0502111].
- [32] J. Lopez Carballo and J. G. Russo, *JHEP*, **0508**, 053 (2005) [arXiv:hep-th/0505226].
- [33] D. R. Brill and M. D. Matlin. *Phys. Rev.*, **D39**, 3151 (1989).
- [34] J. J. Sakurai, *Modern Quantum Mechanics*, Addison-Wesley Publishing Company, New York (1995).
- [35] S. R. Coleman, *Aspects of Symmetry : Selected Erice Lectures*, Cambridge Univ. Press, Cambridge (1988).
- [36] S. R. Coleman and F. De Luccia, *Phys. Rev.*, **D21**, 3305 (1980).
- [37] S. W. Hawking and N. Turok, *Phys. Lett.*, **B425**, 25 (1998) [arXiv:hep-th/9802030].
- [38] J.B. Hartle and S.W. Hawking, *Phys. Rev.*, **D28**, 2960 (1983).
- [39] M. Cvetic and A. A. Tseytlin, *Nucl. Phys.*, **B478**, 181 (1996) [arXiv:hep-th/9606033].
- [40] M. Gutperle and A. Strominger, *JHEP*, **04**, 018 (2002) [arXiv:hep-th/0202210].
- [41] B. Durin and B. Pioline. *Phys. Lett.*, **B625**, 291, (2005) [arXiv:hep-th/0507059].
- [42] Jin-Ho Cho and Philiial Oh, *Phys. Rev.*, **D64**, 106010 (2001) [arXiv:hep-th/0105095].
- [43] Jin-Ho Cho and Philiial Oh, *JHEP*, **0301**, 046 (2003) [arXiv:hep-th/0212009].
- [44] B. Chen, models,” *Phys. Lett.*, **B632**, 393 (2006) [arXiv:hep-th/0508191].
- [45] G. T. Horowitz and K. Maeda. *Class. Quant. Grav.*, **19**, 5543 (2002) [arXiv:hep-th/0207270].
- [46] I. Zlatev, L. M. Wang and P. J. Steinhardt, *Phys. Rev. Lett.*, **82**, 896 (1999) [arXiv:astro-ph/9807002].
- [47] C. Armendariz-Picon, V. F. Mukhanov and P. J. Steinhardt, *Phys. Rev.*, **D63**, 103510 (2001) [arXiv:astro-ph/0006373].
- [48] A. D. Linde. *Phys. Lett.*, **B200**, 272 (1988).
- [49] Soonkeon Nam, *JHEP*, **0003**, 005 (2000) [arXiv:hep-th/9911104].
- [50] R. H. Brandenberger and C. Vafa, *Nucl. Phys.*, **B316**, 391 (1989).
- [51] A. A. Tseytlin and C. Vafa. *Nucl. Phys.*, **B372**, 443 (1992) [arXiv:hep-th/9109048].

- [52] R. Easther, B. R. Greene, M. G. Jackson, and D. Kabat. *Phys. Rev.*, **D67**, 123501 (2003) [arXiv:hep-th/0211124].
- [53] L. F. Abbott, *Phys. Lett.*, **B150**, 427 (1985).
- [54] J. D. Brown and C. Teitelboim, *Phys. Lett.*, **B195**, 177 (1987).
- [55] J. D. Brown and C. Teitelboim, *Nucl. Phys.*, **B297**, 787 (1988).
- [56] R. Bousso and J. Polchinski, *JHEP*, **0006**, 006 (2000) [arXiv:hep-th/0004134].
- [57] G. W. Gibbons and J. B. Hartle. *Phys. Rev.*, **D42**, 2458, (1990).
- [58] N. Kaloper, J. March-Russell, G. D. Starkman and M. Trodden, *Phys. Rev. Lett.*, **85**, 928 (2000) [arXiv:hep-ph/0002001].
- [59] S. Nasri, P. J. Silva, G. D. Starkman and M. Trodden, *Phys. Rev.*, **D66**, 045029 (2002) [arXiv:hep-th/0201063].
- [60] H. Everett. *Rev. Mod. Phys.*, **29**, 454 (1957).
- [61] B. S. DeWitt and N. Graham, *The Many Worlds Interpretation of Quantum Mechanics*, Princeton Univ. Press, Princeton (1973).
- [62] D. Deutsch, *The Fabric of Reality: The Science of Parallel Universes and Its Implications*, Penguin Books, New York (1997).
- [63] M. J. Duff, G. W. Gibbons and P. K. Townsend, *Phys. Lett.*, **B332**, 321 (1994) [arXiv:hep-th/9405124].
- [64] A. Strominger, *JHEP*, **10**, 034 (2001) [arXiv:hep-th/0106113].
- [65] Y. Fujiwara, S. Higuchi, A. Hosoya, T. Mishima and M. Siino, *Phys. Rev.*, **D44**, 1756 (1991).
- [66] G. Oliveira-Neto, *J. Math. Phys.*, **39**, 443 (1998).
- [67] Jin-Ho Cho and Soonkeon Nam, In preparation.
- [68] T. Ortin, *Gravity and Strings*, Cambridge Univ. Press, Cambridge (2004).